## General Disclaimer

## One or more of the Following Statements may affect this Document

- This document has been reproduced from the best copy furnished by the organizational source. It is being released in the interest of making available as much information as possible.

- This document may contain data, which exceeds the sheet parameters. It was furnished in this condition by the organizational source and is the best copy available.

- This document may contain tone-on-tone or color graphs, charts and/or pictures, which have been reproduced in black and white.

- This document is paginated as submitted by the original source.

- Portions of this document are not fully legible due to the historical nature of some of the material. However, it is the best reproduction available from the original submission.

NASA

Technical Memorandum 78028

# CHARACTERIZATION OF GIGAHERTZ (GHz) BANDWIDTH PHOTOMULTIPLIERS

J. B. Abshire and H. E. Rowe

DECEMBER 1977



National Aeronautics and
Space Administration

**Goddard Space Flight Center**
Greenbelt, Maryland 20771

## BIBLIOGRAPHIC DATA SHEET

| 1. Report No. | 2. Government Accession No. | 3. Recipient's Catalog No. |
|---|---|---|
| TM-78028 | | |

| 4. Title and Subtitle | 5. Report Date |
|---|---|
| Characterization of Gigahertz (GHz) Bandwidth Photomultipliers | December 1977 |
| | 6. Performing Organization Code: 723 |
| 7. Author(s): James B. Abshire and H. Edward Rowe | 8. Performing Organization Report No.: G7802-F5 |
| 9. Performing Organization Name and Address: Goddard Space Flight Center, Greenbelt, Maryland 20771 | 10. Work Unit No.: 506-20-33 |
| | 11. Contract or Grant No. |
| | 13. Type of Report and Period Covered: Technical Memorandum |
| 12. Sponsoring Agency Name and Address: National Aeronautics and Space Administration, Washington, D.C. 20546 | 14. Sponsoring Agency Code |

15. Supplementary Notes

16. Abstract

The average impulse response, root-mean-square (rms) times jitter as a function of signal level, single photoelectron distribution, and multiphotoelectron dark-count distribution have been measured for two static crossed-field and five electrostatic photomultipliers. The optical signal source for the first three of these tests was a 30-picosecond (ps) mode-locked laser pulse at 0.53 $\mu$m. The static crossed-field detectors had 2-photoelectron resolution, less than 200-ps rise times, and rms time jitters of 30 ps at the single photoelectron level. The electrostatic photomultipliers had rise times from 1 to 2.5 nanoseconds, and rms time jitters from 160 to 650 ps at the same signal level. The two static crossed-field photomultipliers had ion-feedback-generated dark pulses to the 50-photoelectron level, whereas one electrostatic photomultiplier had dark pulses to the 30-photoelectron level.

| 17. Key Words (Selected by Author(s)) | 18. Distribution Statement |
|---|---|
| Photomultiplier measurement systems, High-speed photomultipliers, Static crossed-field photomultiplier | STAR Category 35<br>Unclassifed–Unlimited |

| 19. Security Classif. (of this report) | 20. Security Classif. (of this page) | 21. No. of Pages | 22. Price* |
|---|---|---|---|
| Unclassified | Unclassified | 52 | $5.25 |

*For sale by the National Technical Information Service, Springfield, Virginia 22151.

All measurement values are expressed in the International System of Units (SI) in accordance with NASA Policy Directive 2220.4, paragraph 4.

# CHARACTERIZATION OF GIGAHERTZ (GHz) BANDWIDTH PHOTOMULTIPLIERS

James B. Abshire and H. Edward Rowe
Goddard Space Flight Center
Greenbelt, Maryland

## Introduction and Summary

Recently, measurement systems have been described that have sufficient bandwidths to permit accurate characterization of gigahertz (GHz) bandwidth photomultipliers.[1] These systems use 30-picosecond (ps), 0.53-μm pulses from a mode-locked Nd:YAG laser as an optical test source. The timing system can resolve root-mean-square (rms) time jitters of less than 20 ps and uses a fast waveform digitizer and minicomputer for data reduction. This paper describes results of tests performed on two static crossed-field and five fast electrostatic photomultipliers using these measurement systems. The five response statistic measurements included average impulse response, single photoelectron pulse resolution, pulsed gain, rms transit-time jitter versus signal level, and the dark-pulse spectrum.

Test results showed that both static crossed-field photomultipliers have 2-photoelectron pulse-height resolutions, and rise times of approximately 120 ps, the fastest of all photomultipliers tested. The rms time jitter of the two static crossed-field photomultipliers was less than 20 ps for signals greater than 2 photoelectrons. The rms time jitter of the five electrostatic photomultipliers ranged from 75 to 450 ps at this signal level.

The distribution of multiphotoelectron dark-anode pulses showed dark pulses to the 50-photoelectron level for the static crossed-field photomultipliers and to 30 photoelectrons from one of the electrostatic photomultipliers. For precise timing applications with short laser pulses, the static crossed-field photomultipliers showed an improvement in time resolution from a factor of 3 to 20 over conventional electrostatic photomultipliers. However, since their multiphotoelectron dark pulses can damage sensitive postdetection electronics, the effect of these dark pulses must be considered in most applications.

Performance studies of the same two static crossed-field photomultipliers have recently been conducted in independent measurements.[2] These results reported the photomultipliers to have slower response times, lower gains, and less time resolution than those reported here. The differences in these results are due to the wider optical signal sources, the difference in optical wavelengths, using full photocathode versus focused spot illumination, and the types of instrumentation used to characterize the photomultipliers. Since ultrashort light pulses and sensitive gigahertz bandwidth instrumentation are manditory to accurately characterize these gigahertz bandwidth photomultipliers, we believe our results more accurately reflect the true device characteristics.

## Description of Photomultipliers Tested

Two Varian static crossed-field photomultipliers were tested. The 154A/1.6L is a six-stage device with an InGaAsP photocathode that has an extended infrared spectral response. The 154D.6D is a similar device, but with a conventional S-20

photocathode. The first and second dynodes of both photomultipliers were coated with GaP (Cs), whereas the remainder of the dynodes were coated with BeO.* The 154A/1.6L was tested with the photocathode at a negative 3650 volts and a positive 580 volts on the electron multiplier focusing rail. The 154D.6D was tested with a photocathode at a negative 3300 volts and a positive 820 volts on the focusing rail. These voltages were found experimentally to give the fastest impulse response to the mode-locked laser pulse. Both photomultipliers have integral voltage-divider networks for dynode biasing and a coaxial anode output connection.

Five electrostatic photomultipliers were tested. Two of these were Amperex 56TVP's that had fourteen Ag-Mg-O(Cs) dynodes and S-20 photocathodes (Reference 3). These photomultipliers were tested with a positive 20 volts at the gating grid and 2500 volts at the anode. The dynode chain used with both 56TVP's was specially designed for use in pulsed laser timing applications. A schematic diagram of this dynode chain is shown in figure 1.

Two RCA 4836 photomultipliers with S-20 photocathodes and ten BeO dynodes were also tested. The RCA 4836 (serial number 8-V-97) was tested with the photocathodes at a negative 1680 volts, whereas the RCA 4836 (serial number 8-V-99) was tested at a negative 1690 volts. RCA had reported that these voltages give a multiplier gain of $1.25 \times 10^5$ for each photomultiplier.[4] The schematic diagram of the dynode chain used for this type of photomultiplier in the tests is shown in figure 2.

*Varian 154A/1.6L and Varian 154D.6D data sheets.

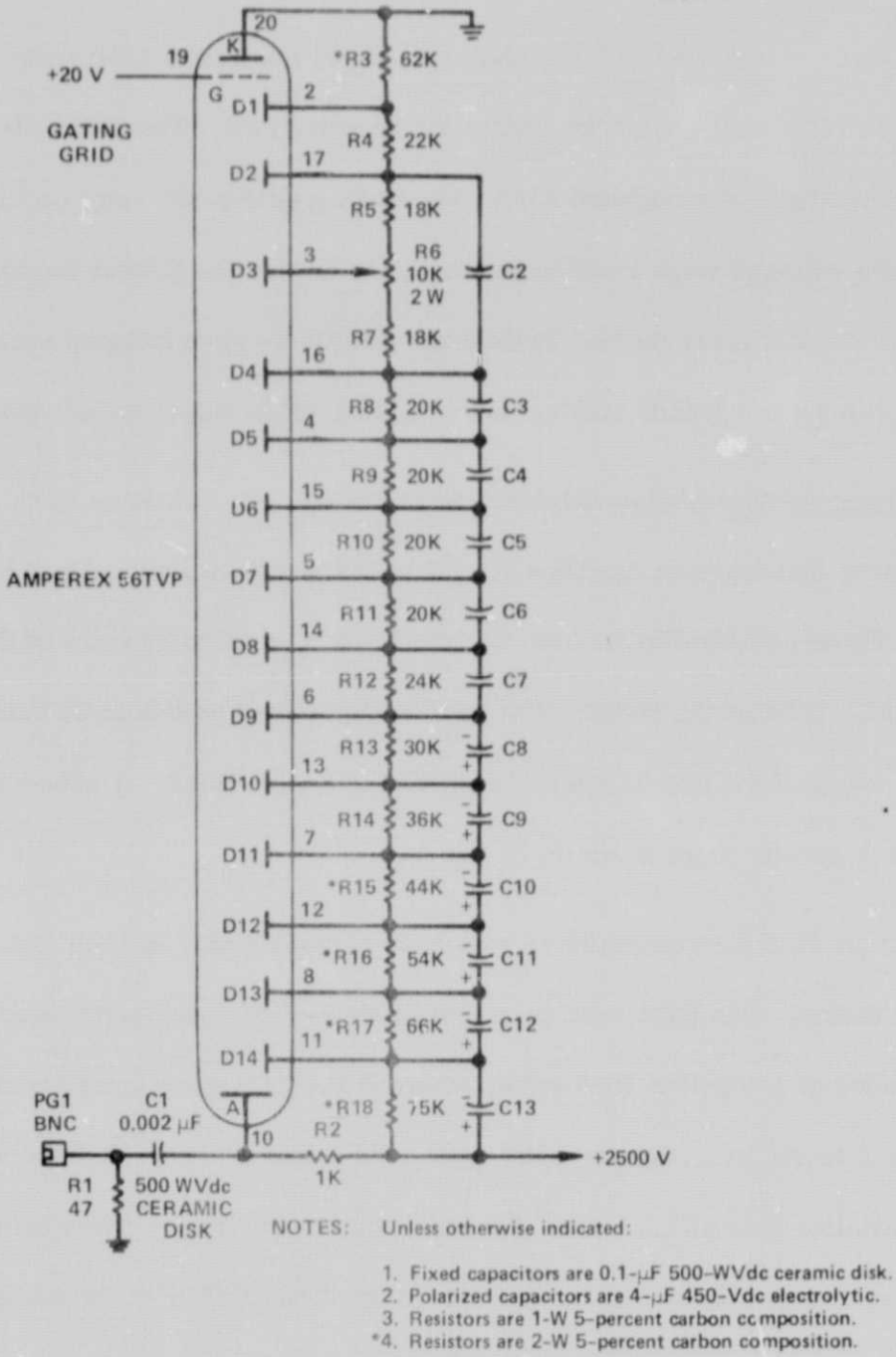


Figure 1. Schematic Diagram of Dynode Chain Used for the Amperex 56TVP Photomultiplier

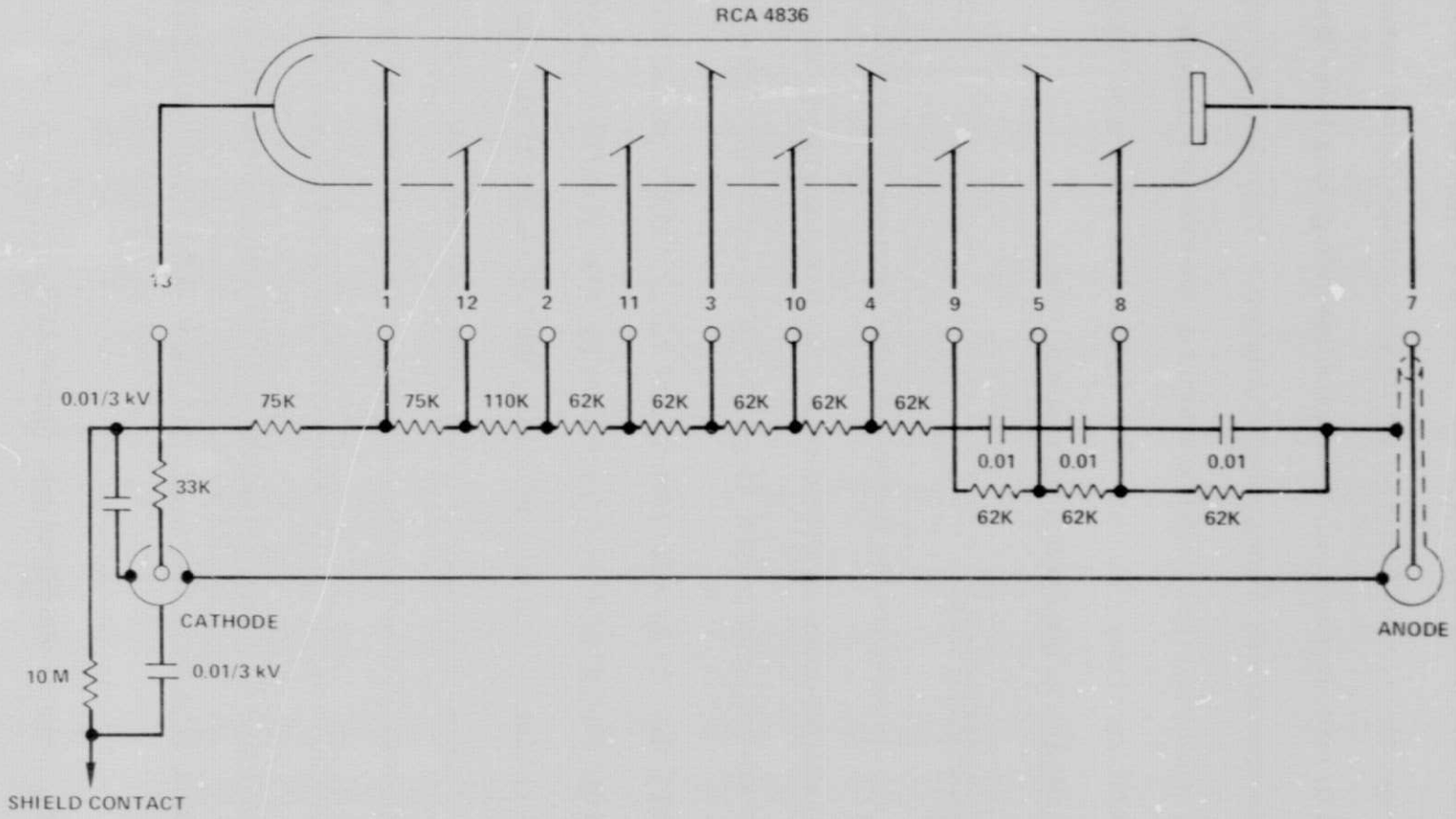


Figure 2. Schematic Diagram of Dynode Chain Used for the RCA 4836 Photomultiplier

One Varian 152S.10P photomultiplier was also tested. This unit has a GaAsP (Cs) photocathode for high quantum efficiency at 0.53 μm and ten BeO dynodes. This photomultiplier was tested with the photocathode at a negative 3150 volts for an electron multiplication gain of $10^6$, with the integral voltage divider connected as recommended by the manufacturer. This operating voltage was lower than optimum for this electrostatically focused photomultiplier.* Therefore, the reported test results show suboptimum performance characteristics for this detector. Higher pulse-height resolution, higher gain, and lower transit-time jitter would be expected when this photomultiplier is operated at its nominal voltage.

Impulse-Response Measurements

The system used to measure the average impulse response of the photomultipliers (figure 3) was described in Reference 1. The 0.53-μm pulses used as optical test sources are estimated to have 30-ps rise times and 50-ps widths.

Figures 4 and 5 show the impulse response of Varian 154A/1.6L and 154D.6D, respectively. These photographs were taken directly from an oscilloscope that houses the sampling plug-ins and thus did not use the minicomputer shown in figure 3. The photographs show that the Varian 154A/1.6L has a 10- to 90-percent rise time of 150 ps and a full width at half-maximum (FWHM) of 160 ps. Similar measurements for the Varian 154D.6D show a rise time of 200 ps and a FWHM of 220 ps. Figure 6 shows the impulse response of the Varian 154A/1.6L and represents the average of 100 sampled waveforms taken by the waveform digitizer.

*R. Klein, Varian, private communication, August 1977.

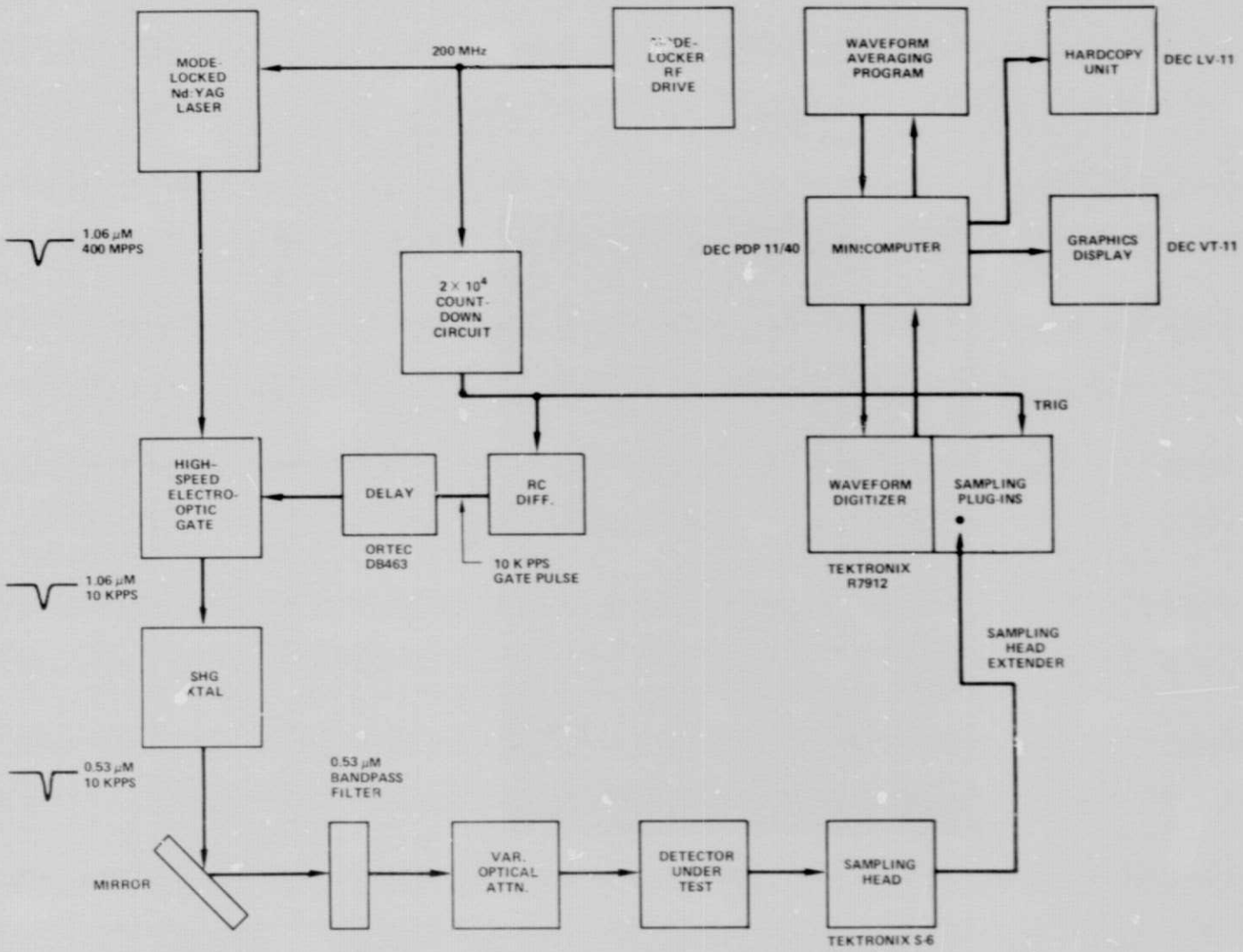


Figure 3. Block Diagram of System for Measuring Detector Average Impulse Response

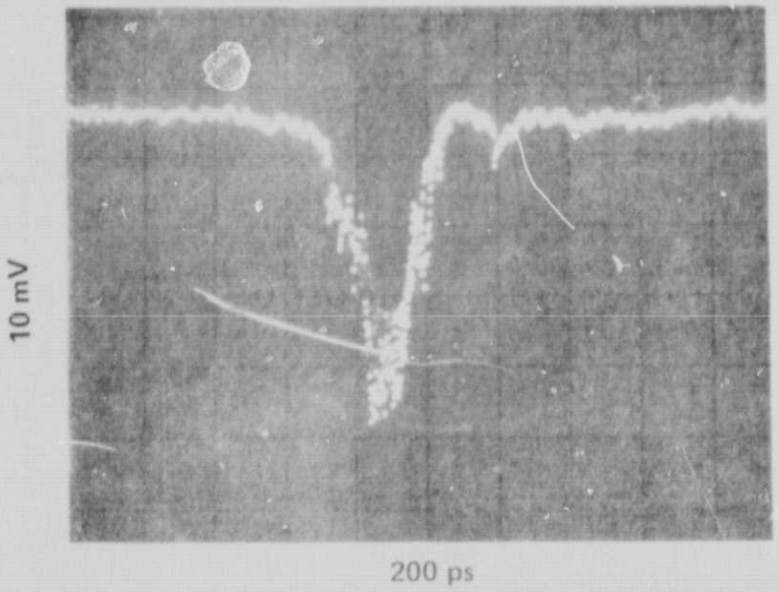


Figure 4. Varian 154A/1.6L Impulse Response

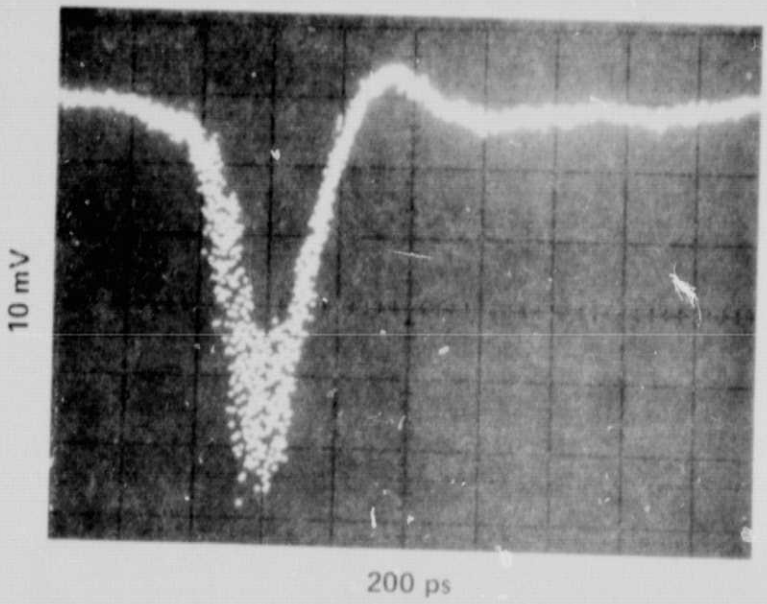


Figure 5. Varian 154D.6D Impulse Response

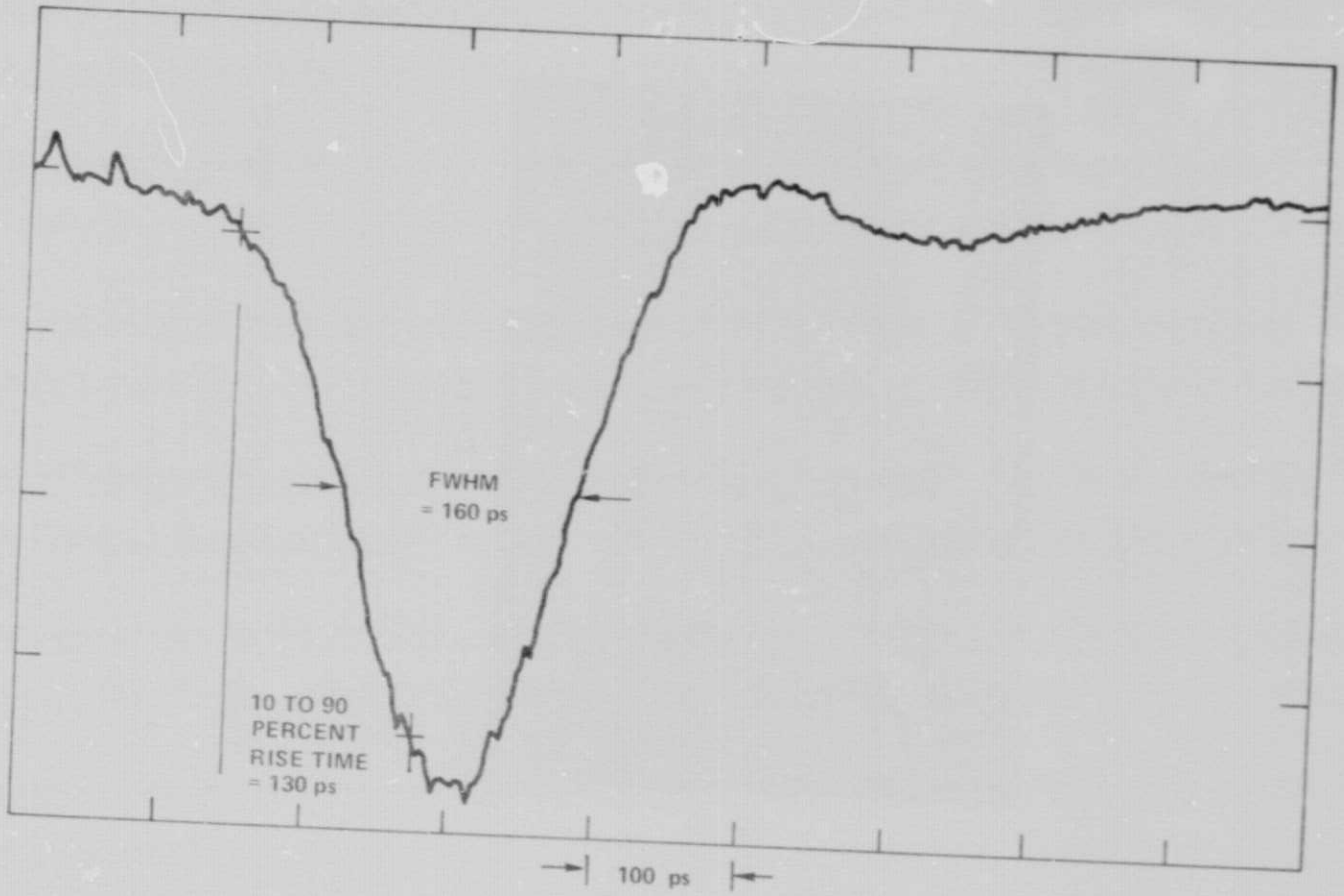


Figure 6. Average Impulse Response of Varian 154A/1.6L

It shows a rise time of 130 ps and FWHM of 160 ps, which agrees with the waveform shown in figure 4.

Figure 7 shows impulse response of the RCA 4836 (serial number 8-V-99). Taken from an oscilloscope as described earlier, this photograph shows a rise time of 2.0 nanoseconds (ns) and pulse width of 2.5 ns FWHM. The after pulses shown were most likely caused by the electrical impedance change from the photomultiplier anode to the external circuitry and sampling head. The impulse response of the second RCA 4836 tested was identical to the one shown in figure 7.

Figure 8 shows the impulse response of the Amperex 56TVP (serial number 31216). This photograph shows that the photomultiplier has a rise time of 2.5 ns and a FWHM of 2.5 ns. Again, an after pulse is clearly evident and was most likely caused by the impedance change from the photomultiplier anode to the external circuitry and sampling head. The impulse response of the Amperex 56TVP (serial number 31223) was identical to the one shown in figure 8.

Figure 9 shows the average impulse response of the Varian 152S.10P (serial number 060). This waveform was the result of averaging 100 individual waveforms from the sampling plug-ins in the waveform digitizer of figure 3. As is shown, the rise time of this detector is 0.95 ns, and the pulse width is 1.2 ns FWHM. The broad tail behind the main pulse was caused by suboptimum focus conditions in the electron optics of the photomultiplier.

Single Photoelectron Pulse-Height Distributions

The single photoelectron pulse-height distribution of a photomultiplier is essentially determined by the multiplication gain of its first dynode. Photomultipliers

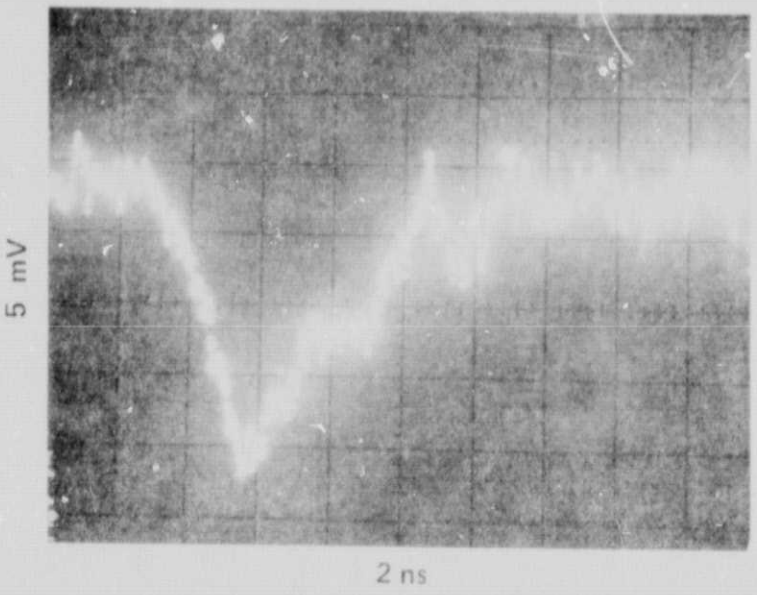


Figure 7. Impulse Response of RCA 4836 (8-V-99)

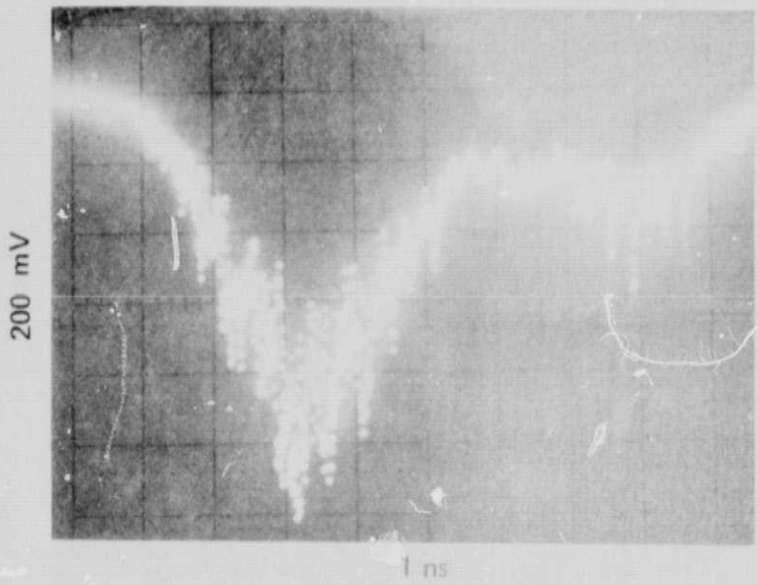


Figure 8. Impulse Response of Amperex 56TVP (31216)

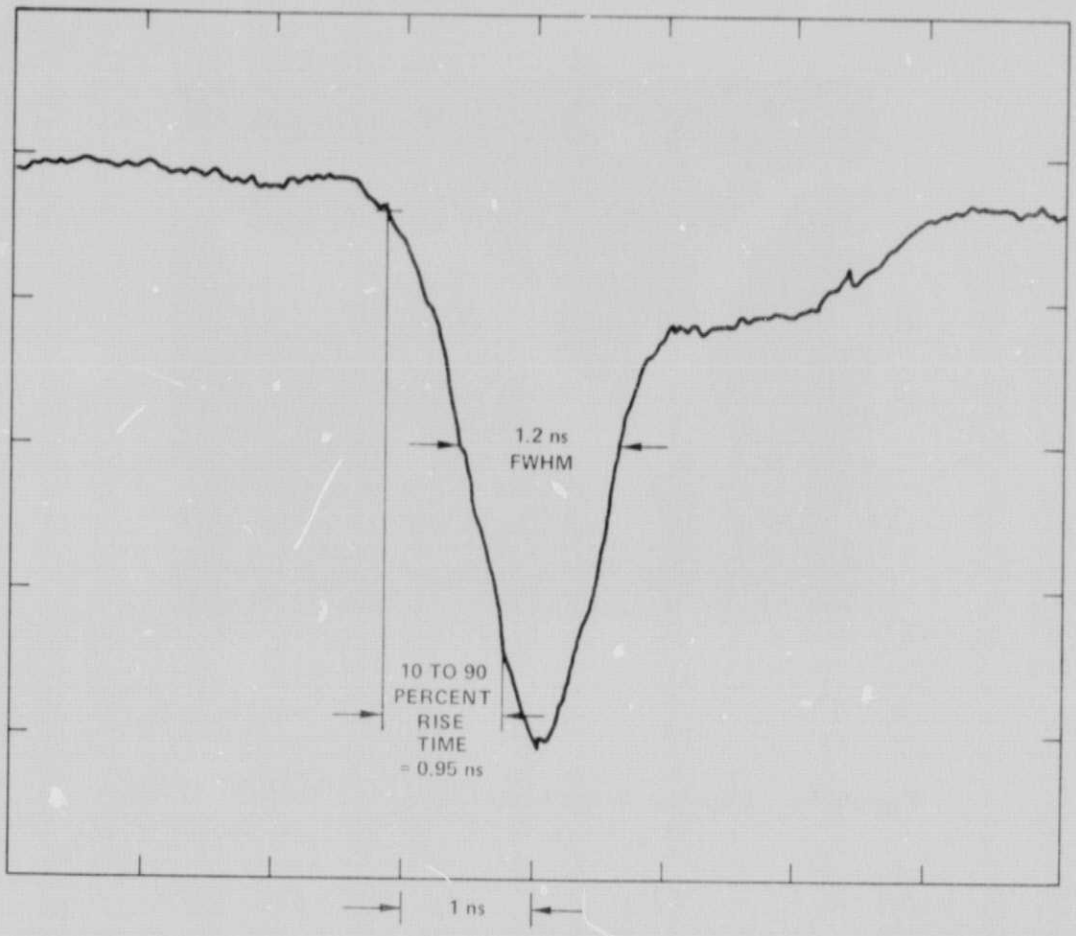


Figure 9. Average Impulse Response of Varian 152S, 10P

that have high-gain first dynodes, such as GaP(Cs), have been shown to have up to 5-photoelectron resolution.[5,6]

The measurement system used for measuring the single photoelectron distribution was described in Reference 1 and is shown in figure 10. This system uses a fast transient digitizer to build histograms of both the photomultiplier output pulse height and the photomultiplier output pulse integral. The optical test source for this system is a 50-ps wide 0.53-μm pulse from a frequency-doubled mode-locked Nd:YAG laser. For each test, the optical beam was focused to a diameter less than 2 millimeters (mm), and was positioned nominally at the center of the photomultiplier photocathode.

Figure 11 shows the pulse-height spectrum and pulse-integral spectrum for the Varian 154A/1.6L. The pulse-height spectrum shows clearly resolved peaks at 1 and 2 photoelectrons, with a single photoelectron voltage of 6.3 millivolts (mV). The pulse-integral spectrum also shows two clearly resolved peaks and shows that the electron multiplication gain of this photomultiplier is $3.5 \times 10^5$. Because the pulse-height and pulse-integral spectrums have similar shapes, the ratio of the pulse height to pulse integral must be very close to a constant. This, in turn, implies that the anode pulse from this photomultiplier has little shape variation at this signal level.

Figure 12 shows the pulse-height spectrum and pulse-integral spectrum for the Varian 154D.6D. Again, the single photoelectron peak is clearly resolved

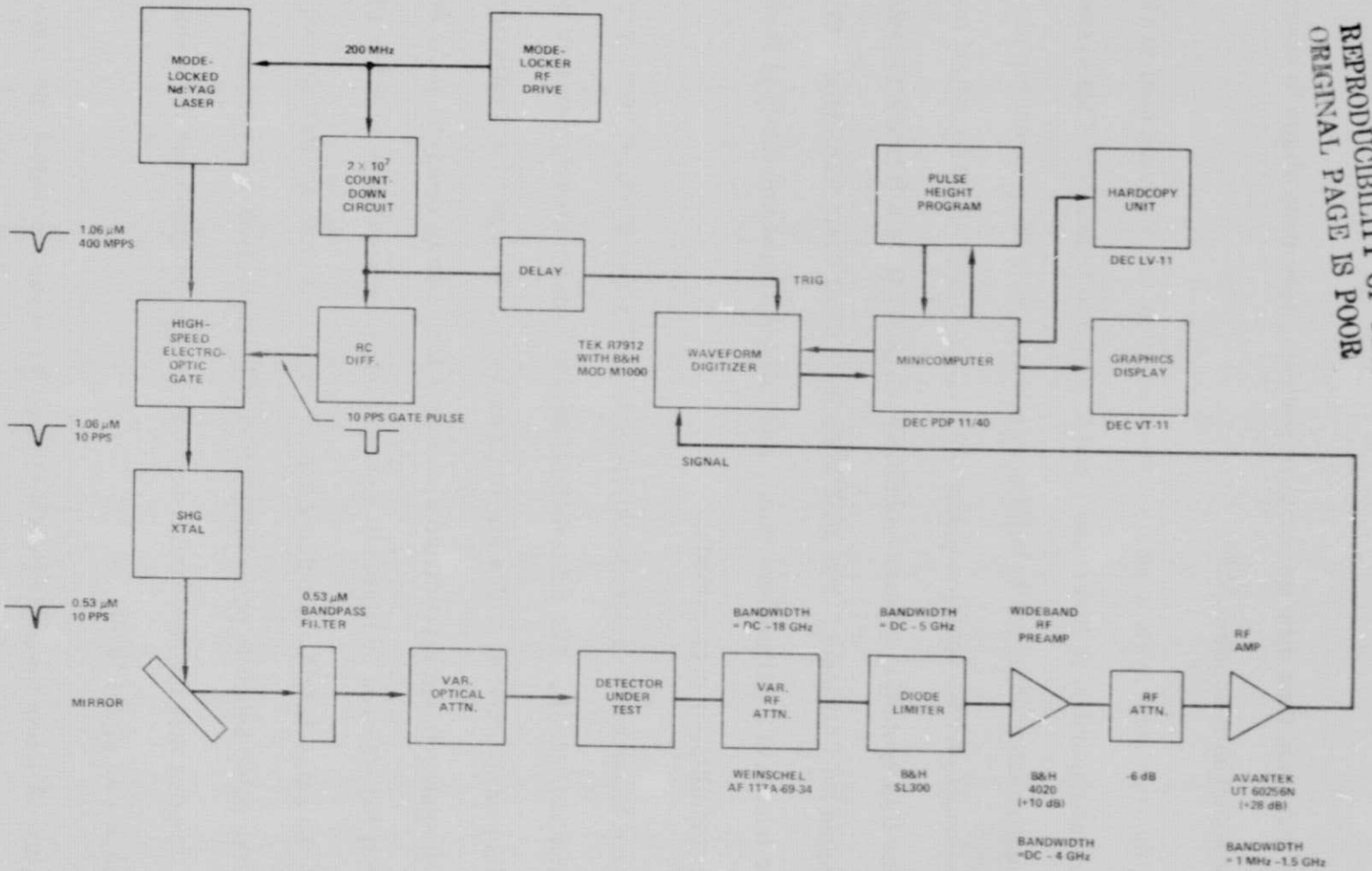


Figure 10. Block Diagram of System for Measuring Detector Pulse-Height Spectrum

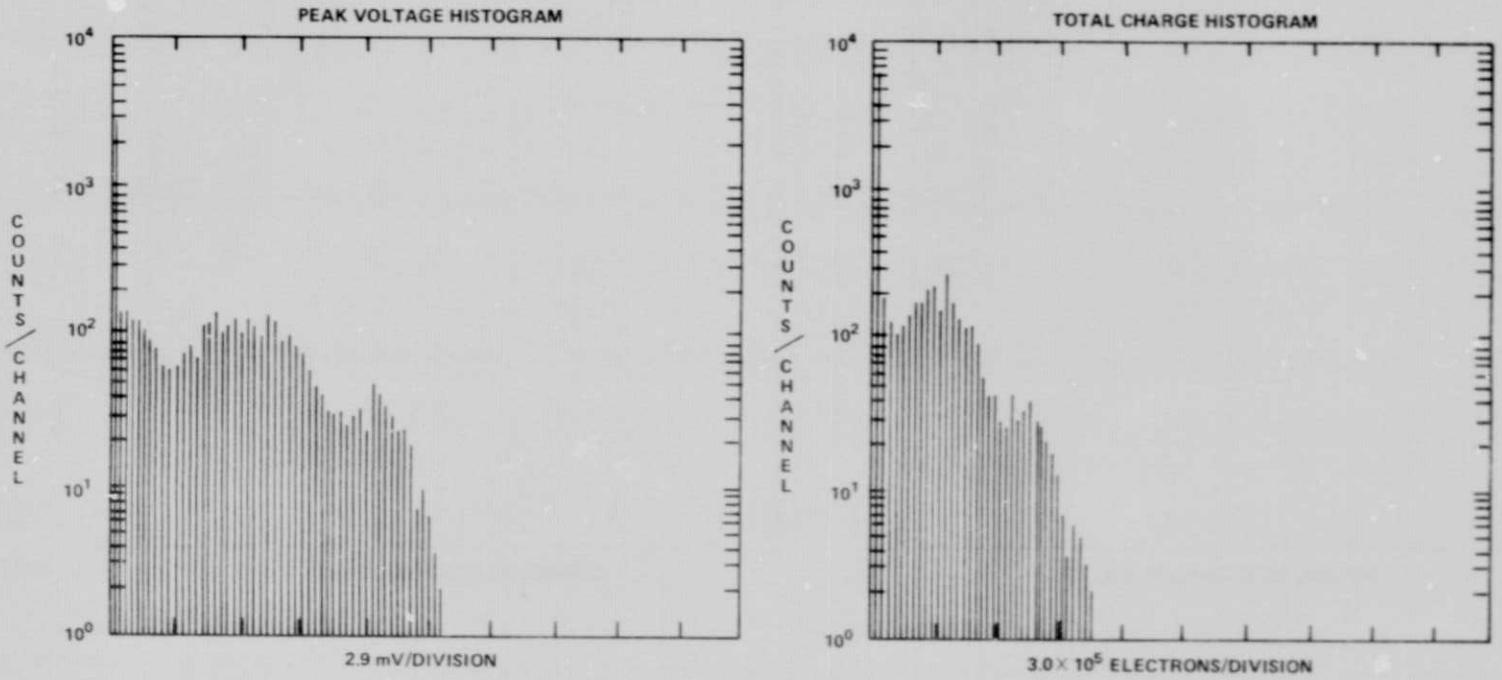


Figure 11. Single Photoelectron Pulse Spectra for Varian 154A/1.6L

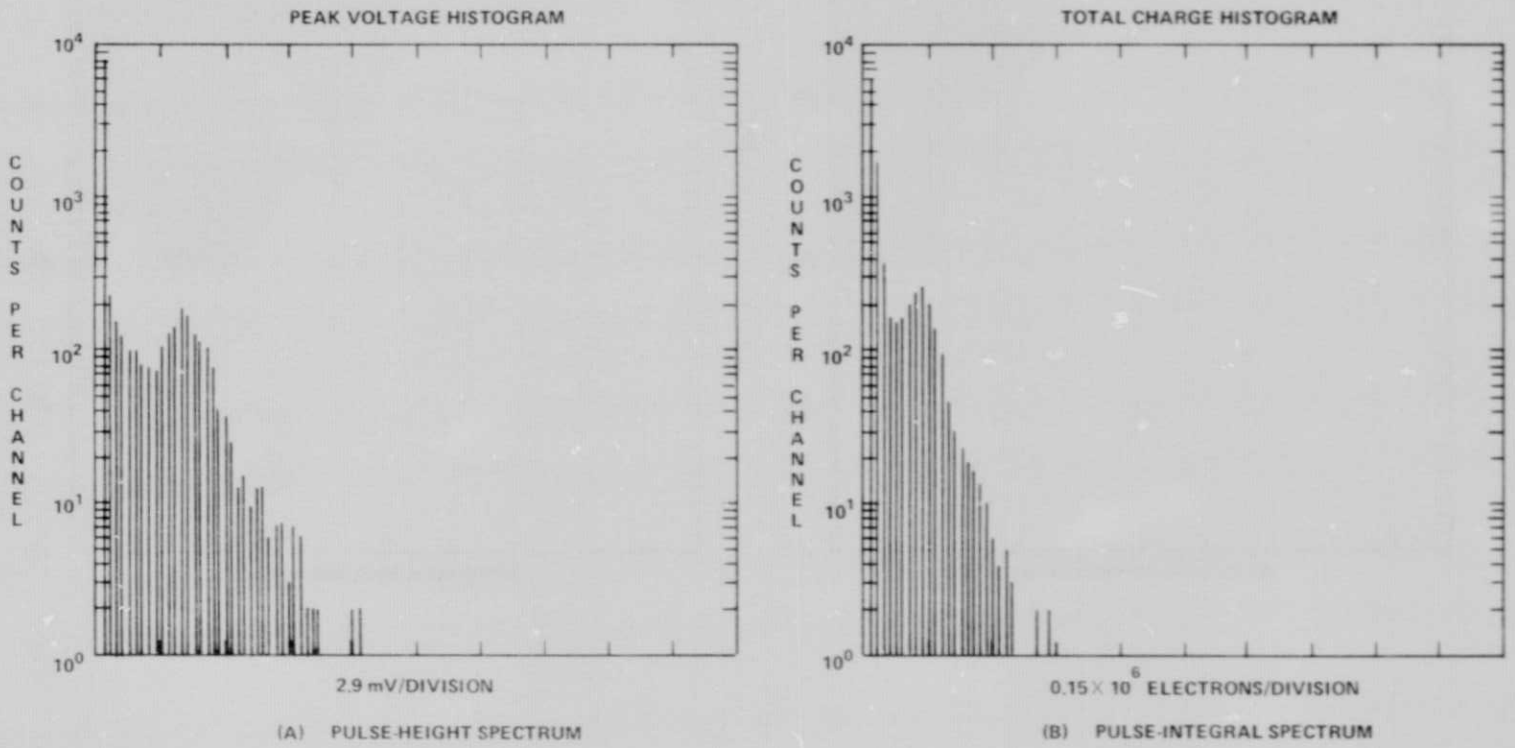


Figure 12. Single Photoelectron Pulse Spectra for Varian 154D, 6D

in both spectra, showing the single photoelectron voltage to be 2.0 mV and the electron multiplication gain to be $1.3 \times 10^5$. Because these data were taken at a lower optical signal level than the previously described results, the 2-photoelectron peak has only a few counts and is not clearly distinquishable.

Because the static crossed-field photomultipliers are identical except for their photocathode materials, the gain and single photoelectron distributions would be expected to be similar. The factor of 3 difference found in their gains is probably attributable to adverse effects of S-20 photocathode processing on the Varian 154D,6D photomultiplier dynode chain.

Figure 13 shows the pulse-height and pulse-integral spectra for the Amperex 56TVP (serial number 31216) photomultiplier. Both distributions are peaked and show the single photoelectron voltage to be 120 mV and the electron multiplication gain to be $4.2 \times 10^7$. Figure 14 shows the corresponding distributions for the Amperex 56TVP (serial number 31223) photomultiplier. Again, both distributions are peaked and show the single photoelectron voltage to be 175 mV and the electron multiplier gain to be $5.5 \times 10^7$. Tests performed at higher signal levels showed no multiple photoelectron resolution for either of the two Amperex 56TVP photomultipliers tested. This is to be expected because the average electron multiplication gain per dynode is only 3.7 for this model photomultiplier.

Figure 15 shows the single photoelectron pulse-height distribution and pulse-integral distribution for the RCA 4836 (serial number 8-V-97) photomultiplier.

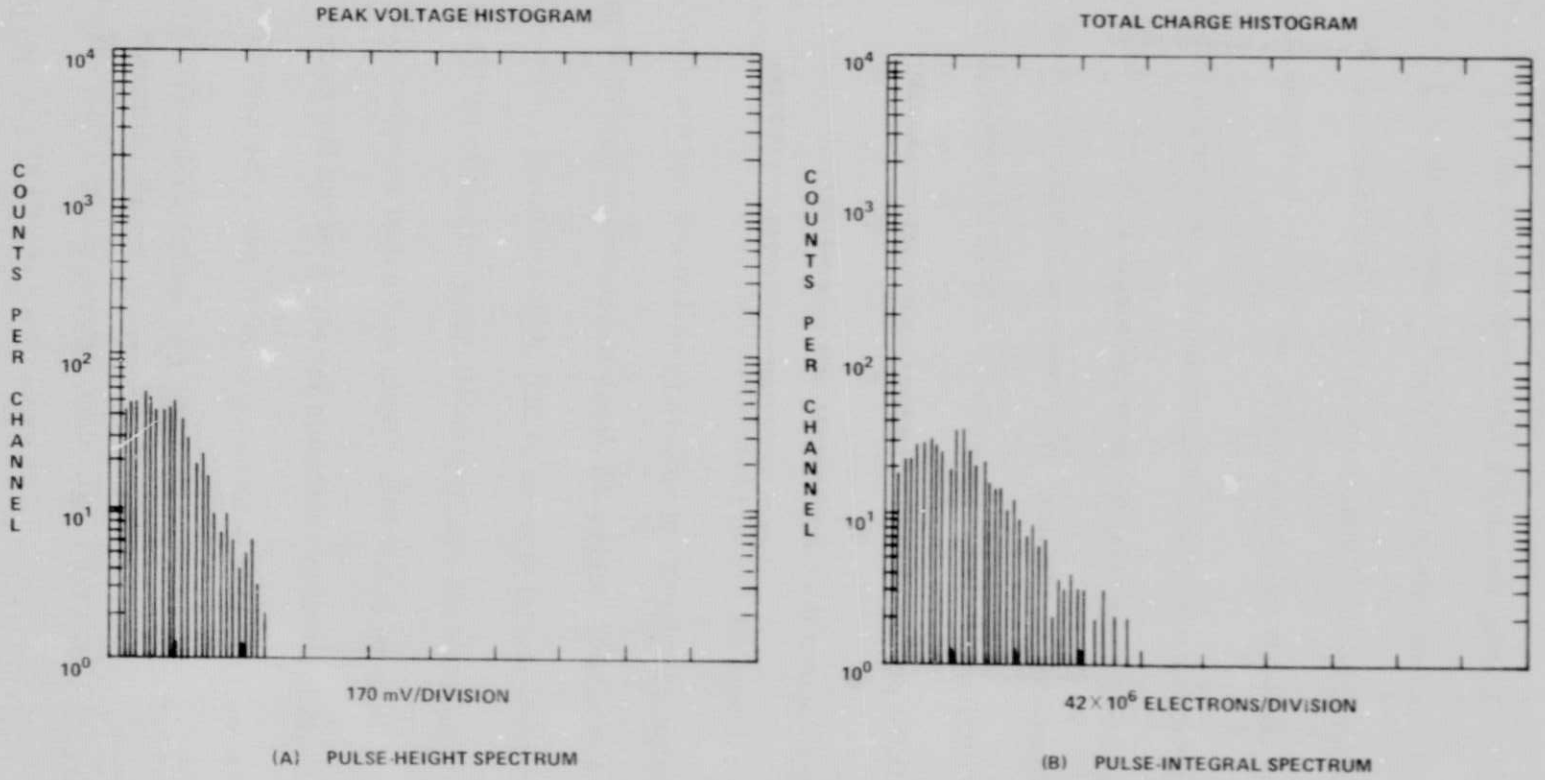


Figure 13. Single Photoelectron Pulse Spectra for Amperex 56TVP (Serial Number 31216)

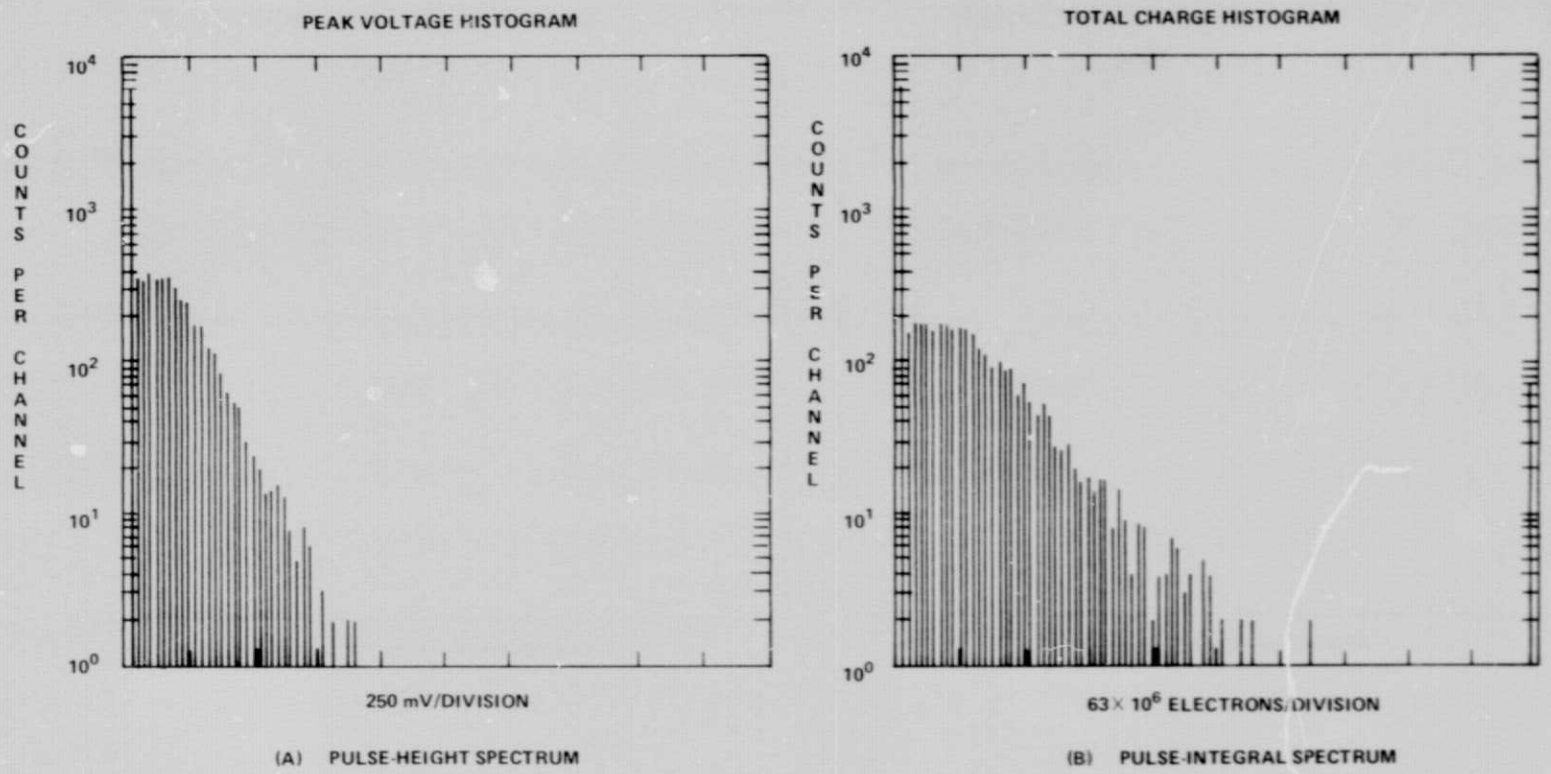


Figure 14. Single Photoelectron Pulse Spectra for Amperex 56TVP (Serial Number 31223)

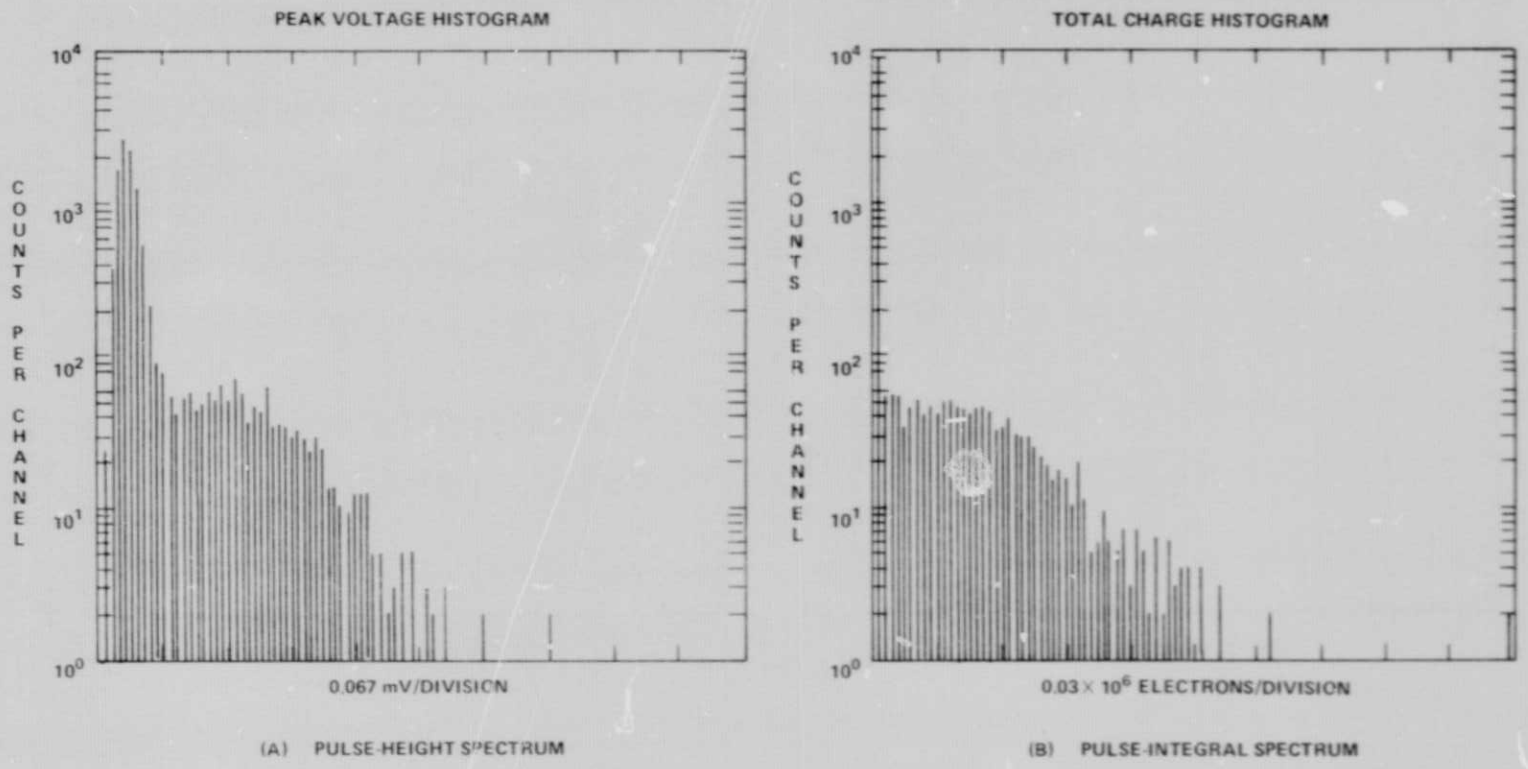


Figure 15. Single Photoelectron Pulse Spectra for RCA 4836 (Serial Number 8-V-97)

The first peak in figure 15a is the peak due to no photoelectrons from the photocathode. The spread in this peak is caused by the additive preamplifier noise in the measurement system. The low gain of both RCA 4836 photomultipliers required large amounts of external amplification, and, hence, the measured histograms are slightly broadened by the noise of the amplifier chain.

The single photoelectron voltage was measured to be 0.15 mV from figure 15a, and the electron multiplier gain was measured to be $4.5 \times 10^4$. Similarly, as shown in figure 16, the single photoelectron voltage was measured to be 0.12 mV for the RCA 4836 (serial number 8-V-99). No peak in the pulse-integral histogram was discernible for this photomultiplier.

Figure 17 shows the pulse-height and pulse-integral distributions for the Varian 152S.10P (serial number 60) photomultiplier. Both distributions are very smooth and are representative of those obtained in testing this photomultiplier. From two small peaks in these distributions and from the dark-count spectra described later in this report, the single photoelectron voltage was estimated to be 6 mV, and the electron multiplier gain was estimated to be $6 \times 10^5$. The poor pulse-height resolution for this photomultiplier suggests that the first dynode has a low electron multiplication gain.

Transit-Time Jitter

Because photomultipliers are often used in precise timing applications, it is important to measure the amount of jitter in the occurrence time of the anode pulse.

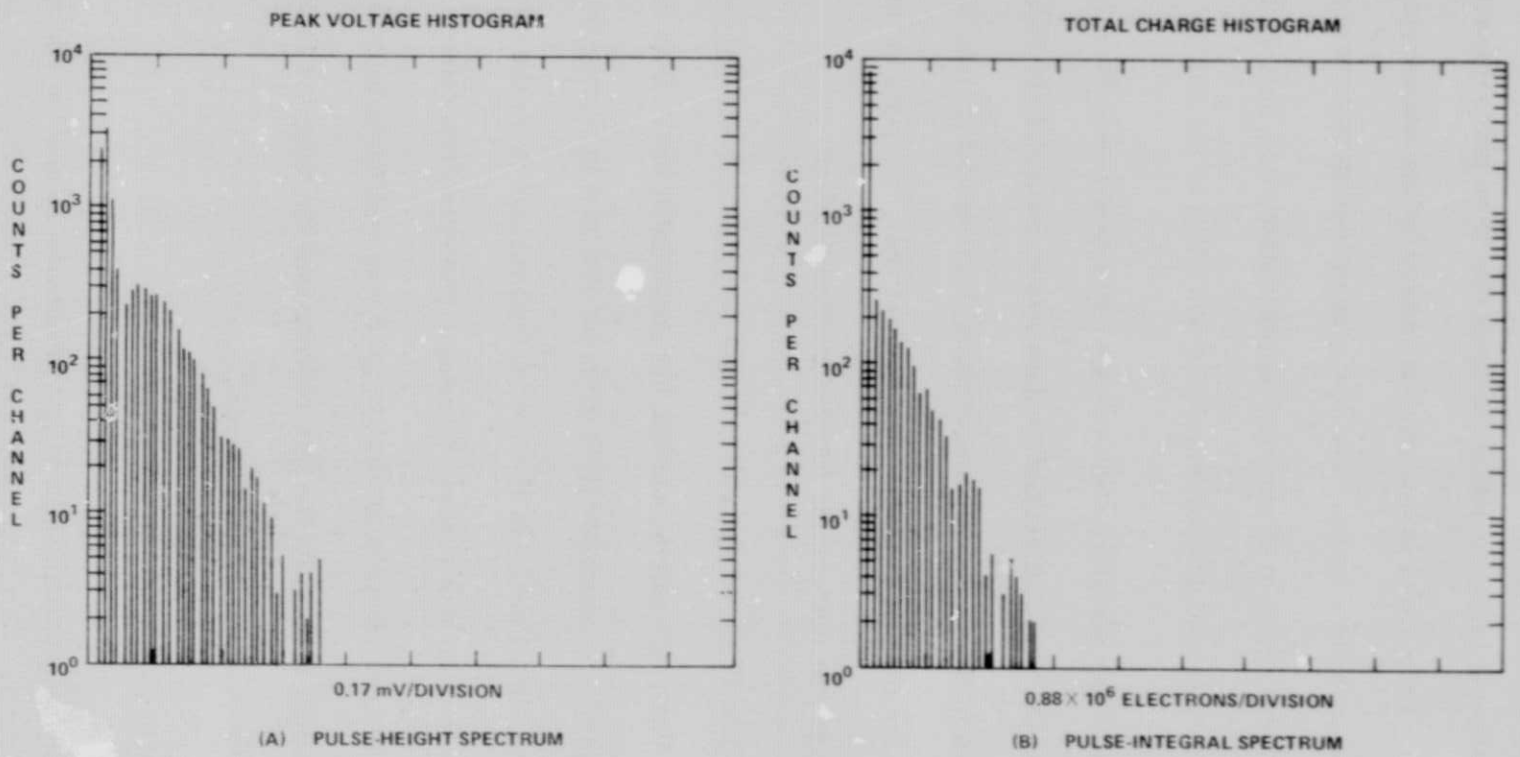


Figure 16. Single Photoelectron Pulse Spectra for RCA 4836 (Serial Number 8-V-99)

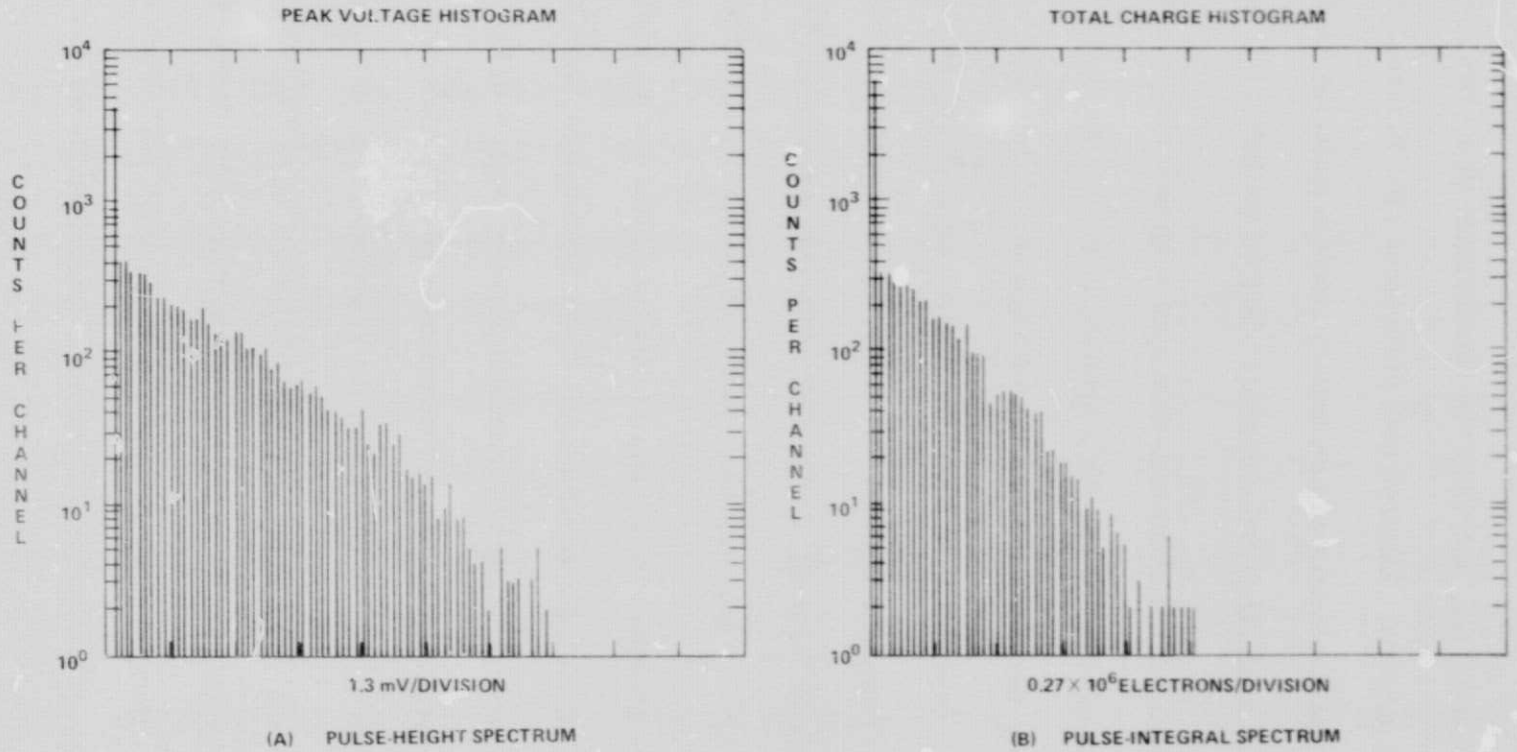


Figure 17. Single Photoelectron Pulse Spectra for Varian 152S.10P

In photomultipliers, this time jitter is usually caused by path differences of the electron trajectories, both from the photocathode to the first dynode, and between successive dynodes. Electron path differences are, in turn, caused both by differences in photoelectron and secondary electron emission locations and by the spread of photoelectron and secondary electron energies.

The photomultiplier transit-time spread measurements were made using the system shown in figure 18. This system, which was described in Reference 1, can measure the mean and rms transit time of a photomultiplier as a function of signal level over the 1- to 100-photoelectron range. The measurement system uses a fast transient digitizer and computes these transit-time statistics for 50-percent rise time, peak, and centroid detection strategies. The optical test source is a short 0.53-μm laser pulse, as previously described.

Figure 19 shows the measured rms time jitter versus signal level for the Varian 154A/1.6L photomultiplier. These transit-time jitter measurements for both static crossed-field photomultipliers were made with the waveform digitizer at its fastest sweep speed of 10 ps per element. At this sweep speed, the system resolution is 15 ps. It shows that the rms time jitter for this photomultiplier was approximately 30 ps at the single photoelectron level and below the measurement system resolution of 15 ps for all signals above the 3-photoelectron level. Of the three detection strategies used in the measurement, none was found to give superior time-resolution performance. Figure 20 shows similar results for

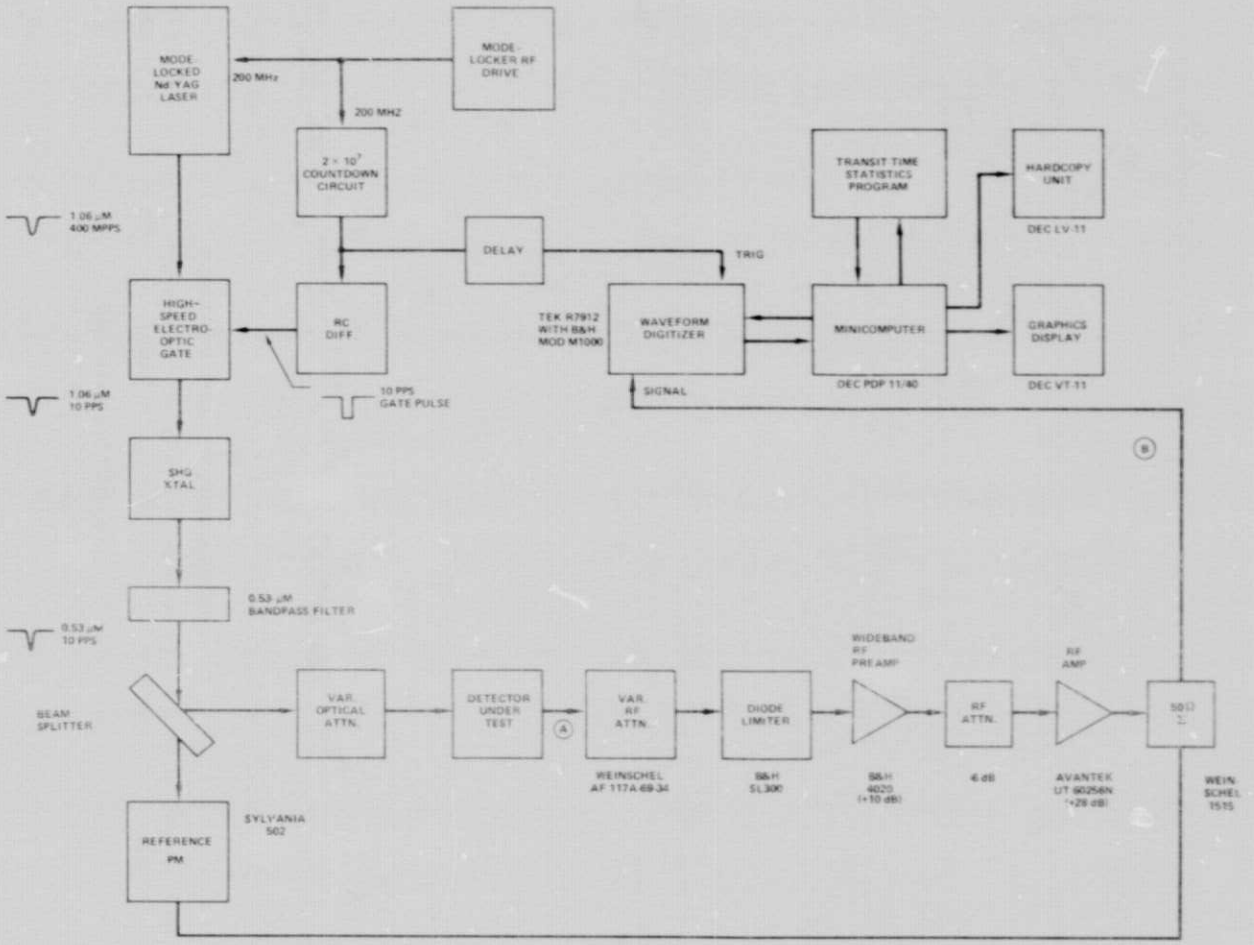


Figure 18. Block Diagram of System for Measuring Detector Transit-Time Statistics

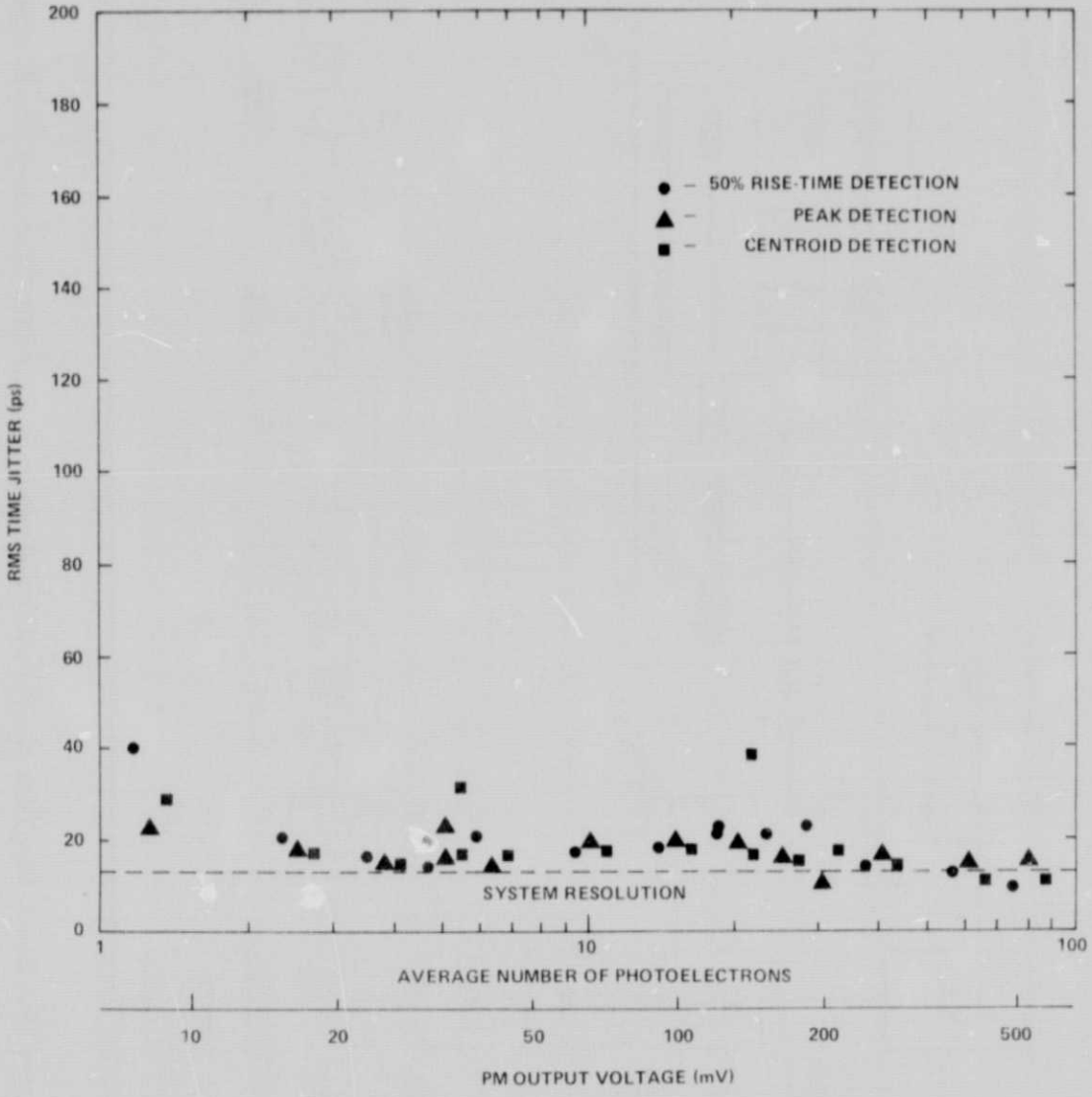


Figure 19. Rms Time Jitter versus Pulse Amplitude for Varian 154A/1.6L with Detection Strategy as a Parameter

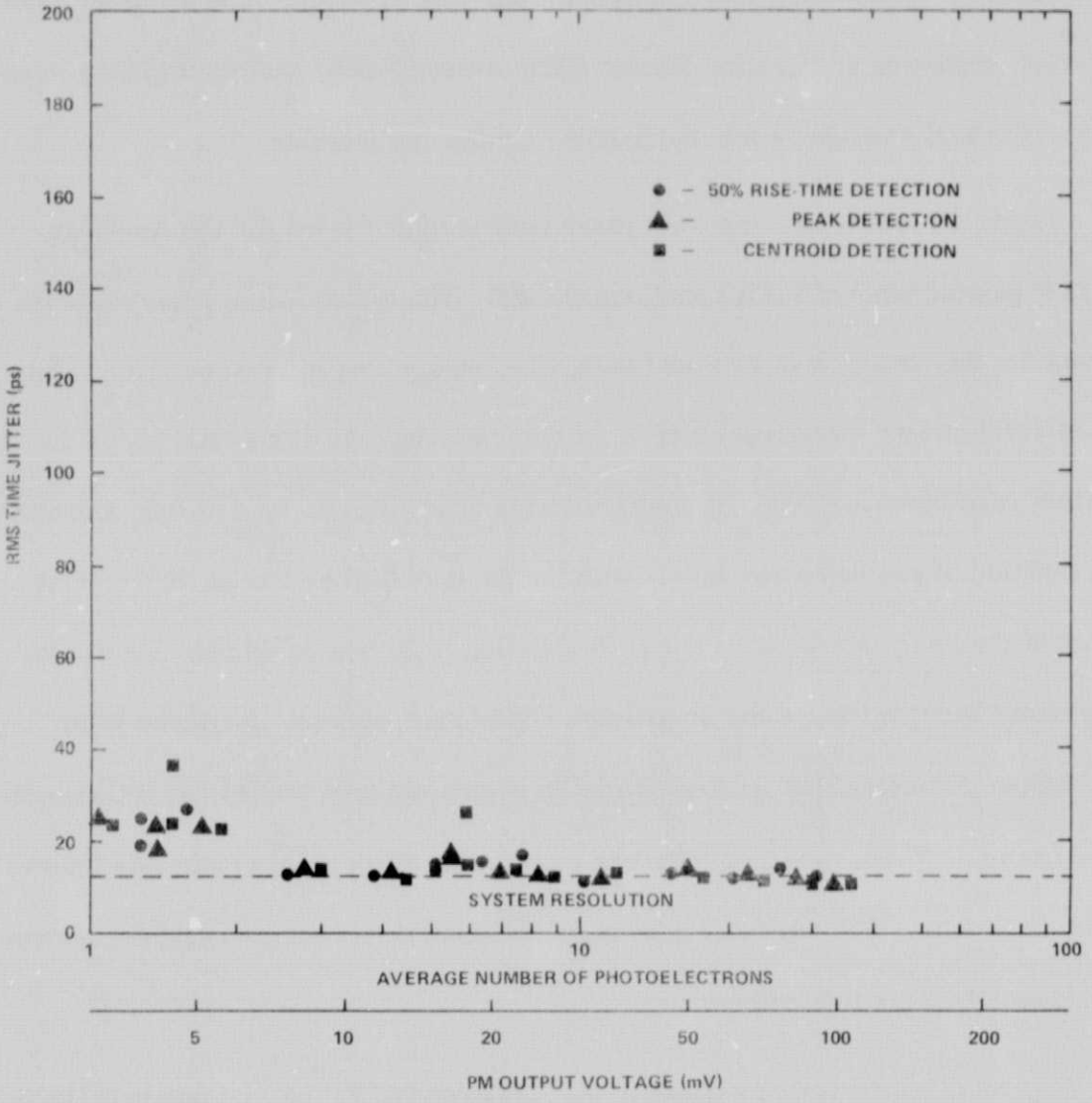


Figure 20. Rms Time Jitter versus Pulse Amplitude for Varian 154D, 6D with Detection Strategy as a Parameter

the Varian 154D.6D photomultiplier. Again, for all signals above 3 photoelectrons, the amount of rms time jitter was below the measurement system resolution, whereas the time jitter at 1-photoelectron was 25 ps. As before, no clearly optimum detection strategy was noticeable for this detector. The excellent transit-time statistics shown here for the static crossed-field photomultipliers make them excellent candidates for short-pulse timing applications.

Figure 21 shows the rms time jitter versus signal level for the Amperex 56TVP (serial number 31216) photomultiplier. The transit-time jitter measurements for the Amperex 56TVP and RCA 4836 photomultipliers were made at a transient digitizer sweep speed of 40 ps per element. At this sweep speed the system resolution is 45 ps. It shows the rms time jitter to be a slowly decreasing function of photoelectron level, with the photomultiplier having 700-ps rms jitter at the one photoelectron level, decreasing to 200-ps at 30 photoelectrons. The error bars represent the 90-percent confidence intervals for these jitter estimates, assuming that the time jitter in each amplitude bucket has a Gaussian distribution. Where no error bars are shown, the 90-percent confidence interval is 40 ps or less. Fifty-percent rise time and peak detection give slightly improved time resolution for this detector.

Figure 22 shows similar data for the Amperex 56TVP (serial number 31223) photomultiplier. Again, the rms time jitter decreases as a function of signal level from 500 ps at 1 photoelectron, to 180 ps at 100 photoelectrons. There was

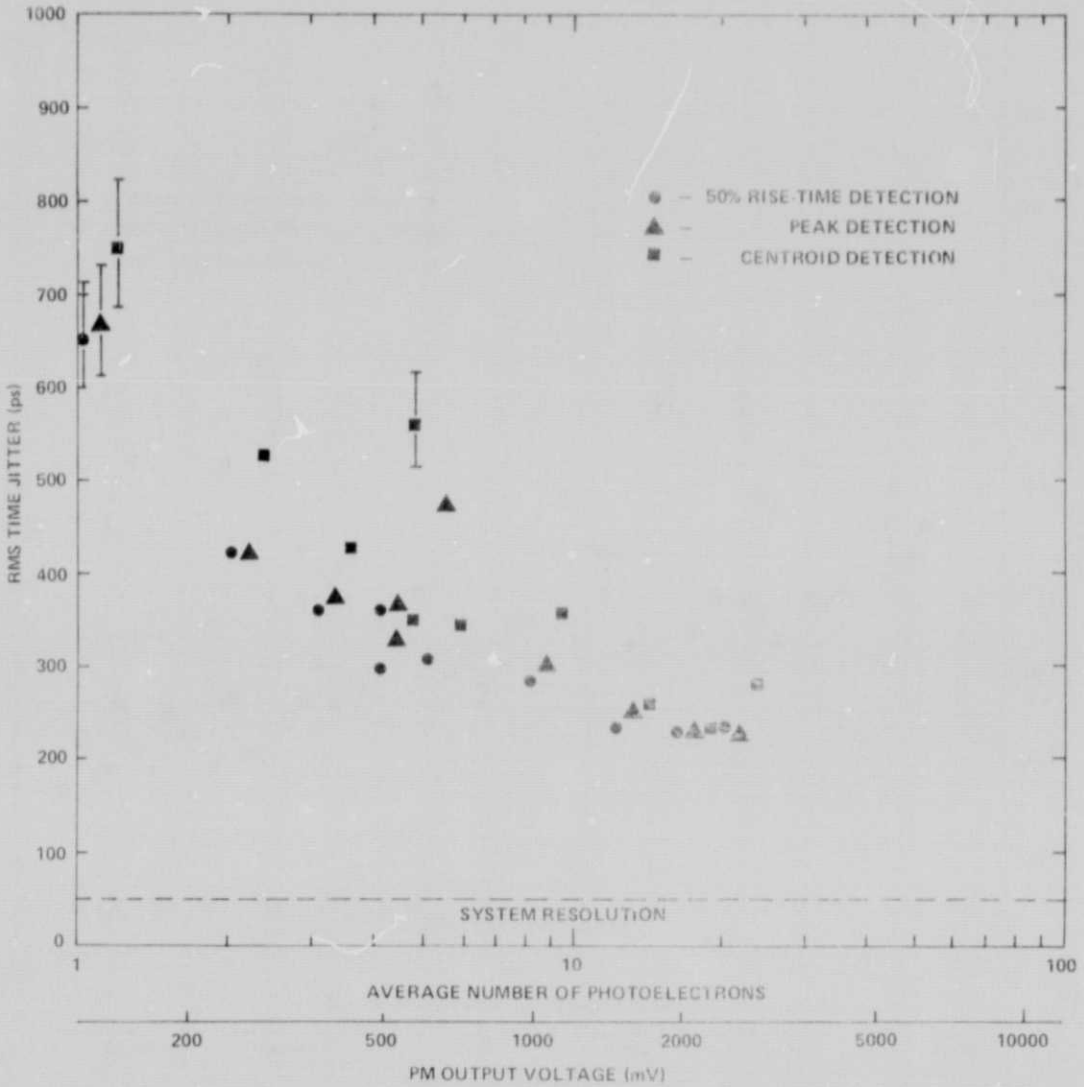


Figure 21. Rms Time Jitter versus Pulse Amplitude for Amperex 56TVP (Serial Number 31216) with Detection Strategy as a Parameter

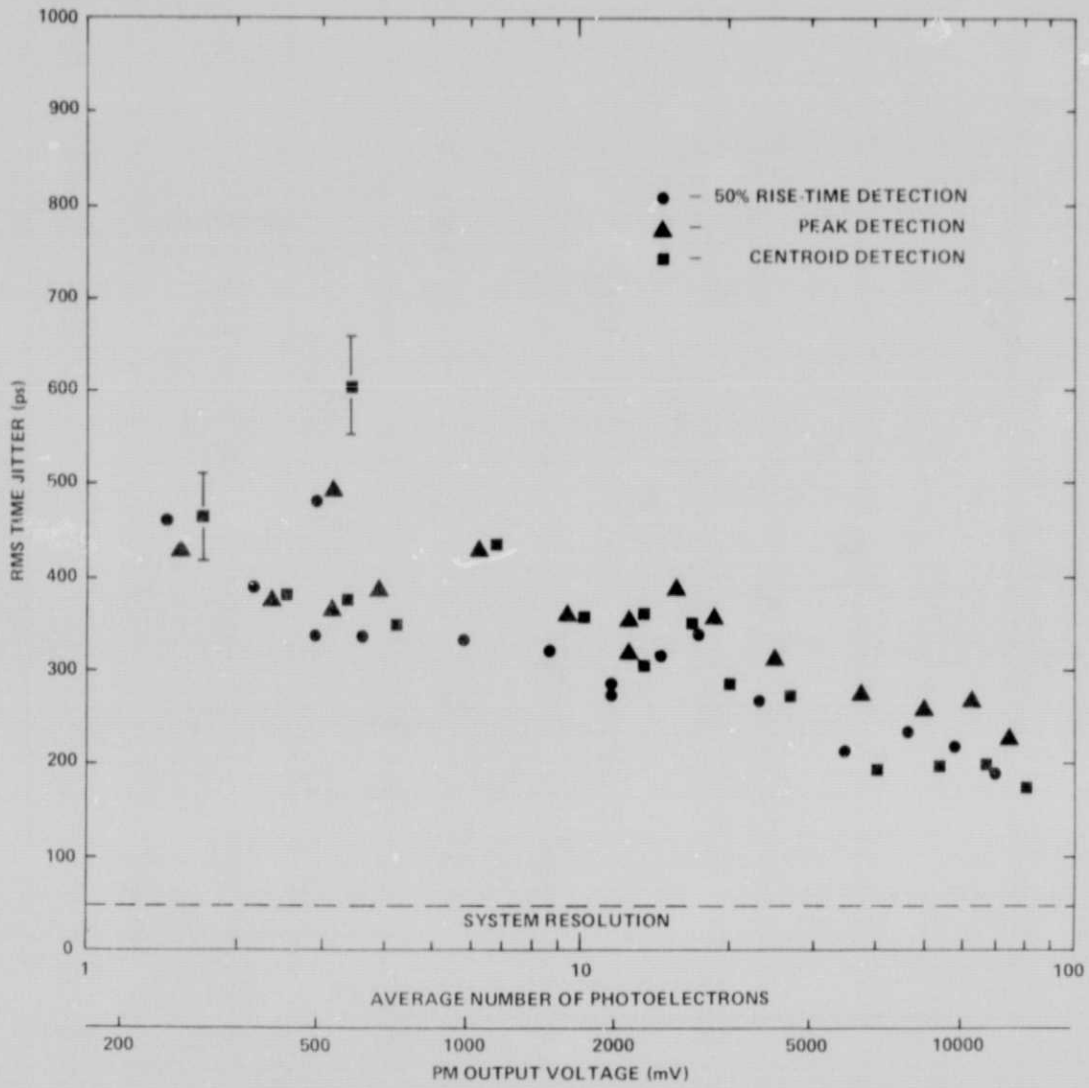


Figure 22. Rms Time Jitter versus Pulse Amplitude for Amperex 56TVP (Serial Number 31223) with Detection Strategy as a Parameter

no clearly optimum detection strategy for reducing the rms time jitter among the three tested for this detector. The slow decrease of time jitter with increased signal level was most likely caused by both the large number of dynodes and the large multiplier transit-time delay for this photomultiplier. These conditions could produce significant electron-path differences within the electron multiplier structure and could account for the very random output-pulse shapes noted for the photomultiplier during testing.

Figure 23 shows the measured rms time jitter versus signal level for the RCA 4836 (serial number 8-V-97). The data show the rms time jitter to be 425 ps at 2 photoelectrons, with the time jitter decreasing to 75 ps at 35 photoelectrons. Figure 24 shows similar data for the RCA 4836 (serial number 8-V-99) photomultiplier. It shows the rms time jitter to be 310 ps at the 2-photoelectron level, decreasing to 40 ps at the 100-photoelectron level. The 50-percent rise time and peak detection strategies gave the least time jitter of the detection strategies tested.

Because both RCA 4836 photomultipliers have relatively low gains and wide impulse responses, all available preamplifier gain was used in the measurement system when testing these photomultipliers. Therefore, the time jitter measured at low photoelectron levels was significantly increased by the residual system preamplifier noise. The poor performance of centroid detection, as compared

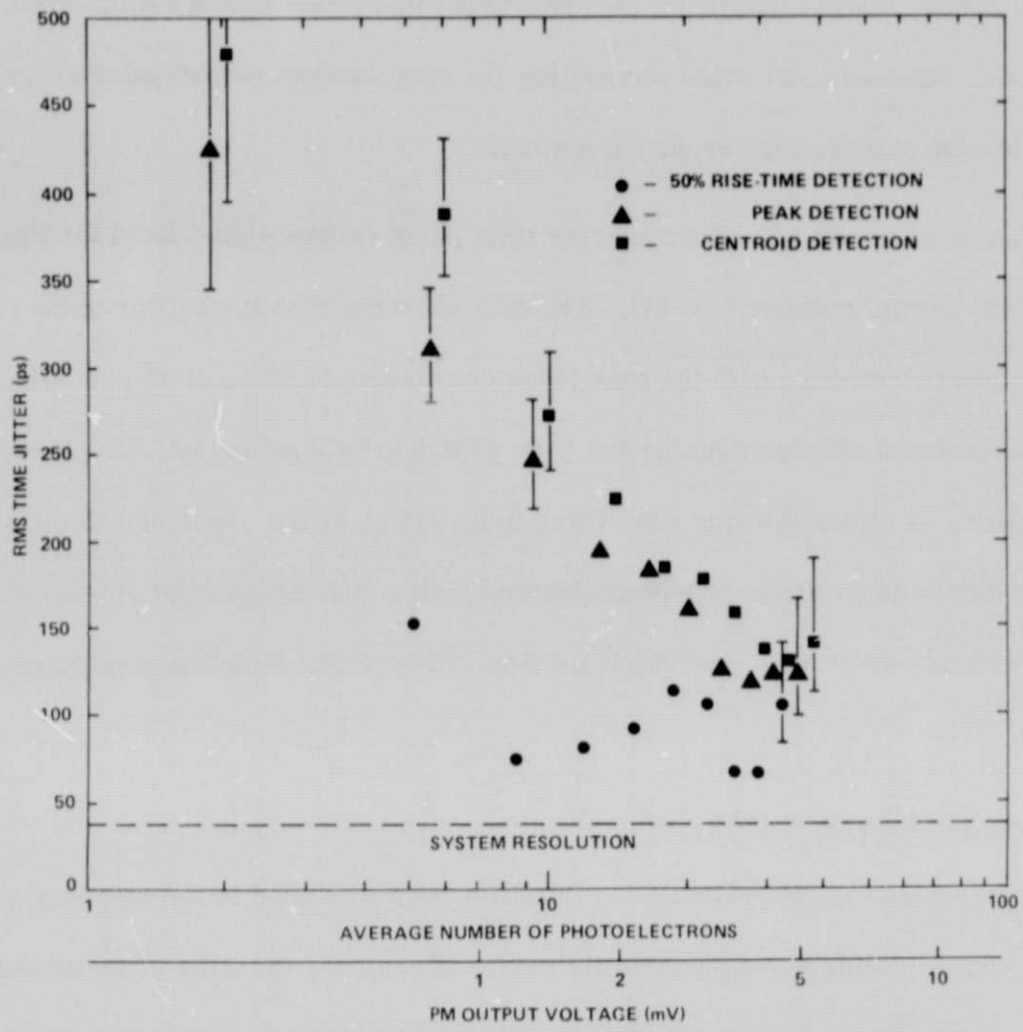


Figure 23. Rms Time Jitter versus Pulse Amplitude for RCA 4836 (Serial Number [illegible]-V-97) with Detection Strategy as a Parameter

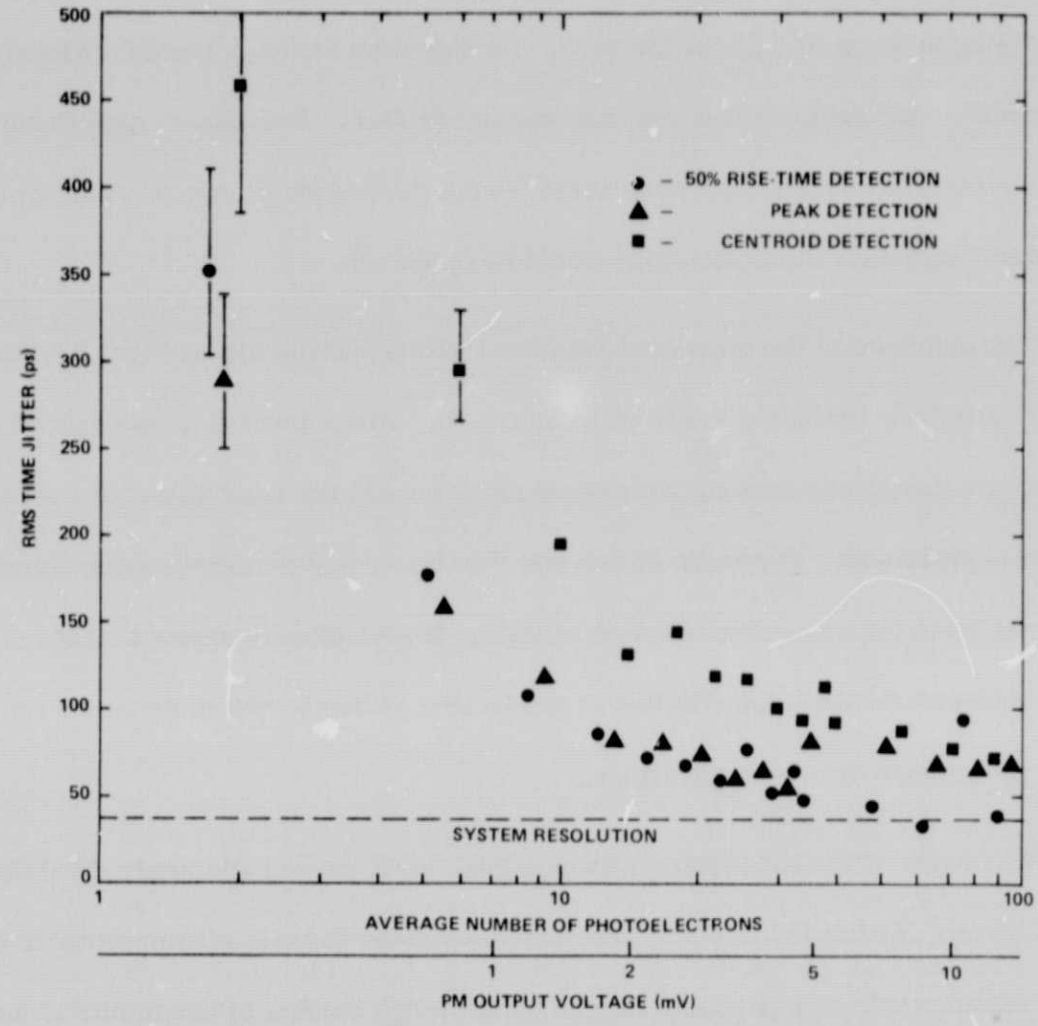


Figure 24. Rms Time Jitter versus Pulse Amplitude for RCA 4836 (Serial Number 8-V-99) with Detection Strategy as a Parameter

to 50-percent rise time and peak detection, was probably caused by the effects of this system noise on the time-jitter measurements.

Figure 25 shows the rms time jitter versus signal level for the Varian 152S.10P photomultiplier. These time-jitter measurements were made at a sweep speed of 20 ps per sampling element, where the system resolution is 25 ps. Figure 25 shows the time jitter to be approximately 160 ps at 1 photoelectron, decreasing to 55 ps at 5 photoelectrons. No detection strategy tested obviously improved timing performance for this photomultiplier. Because no significant anode pulse-shape variations were noted during the testing of this photomultiplier, no clearly optimum timing strategy would be expected.

A comparison of the measured rms time jitters versus signal level for the photomultipliers evaluated is shown in figure 26. When more than one photomultiplier of a model was tested, the photomultiplier with the least jitter was selected for the comparison. Figure 26 shows that the time jitter is a decreasing function of signal level for all photomultiplier models. It also clearly shows that the static crossed-field photomultiplier is preferable of those photomultipliers evaluated for precise-timing applications.

The slopes of the time-jitter versus signal-level curves are approximately equal, except for the RCA 4836. The increased slope for this photomultiplier for small signal levels was probably caused by the large amount of preamplifier noise present in the measuring system. Because the amount of additive amplifier noise

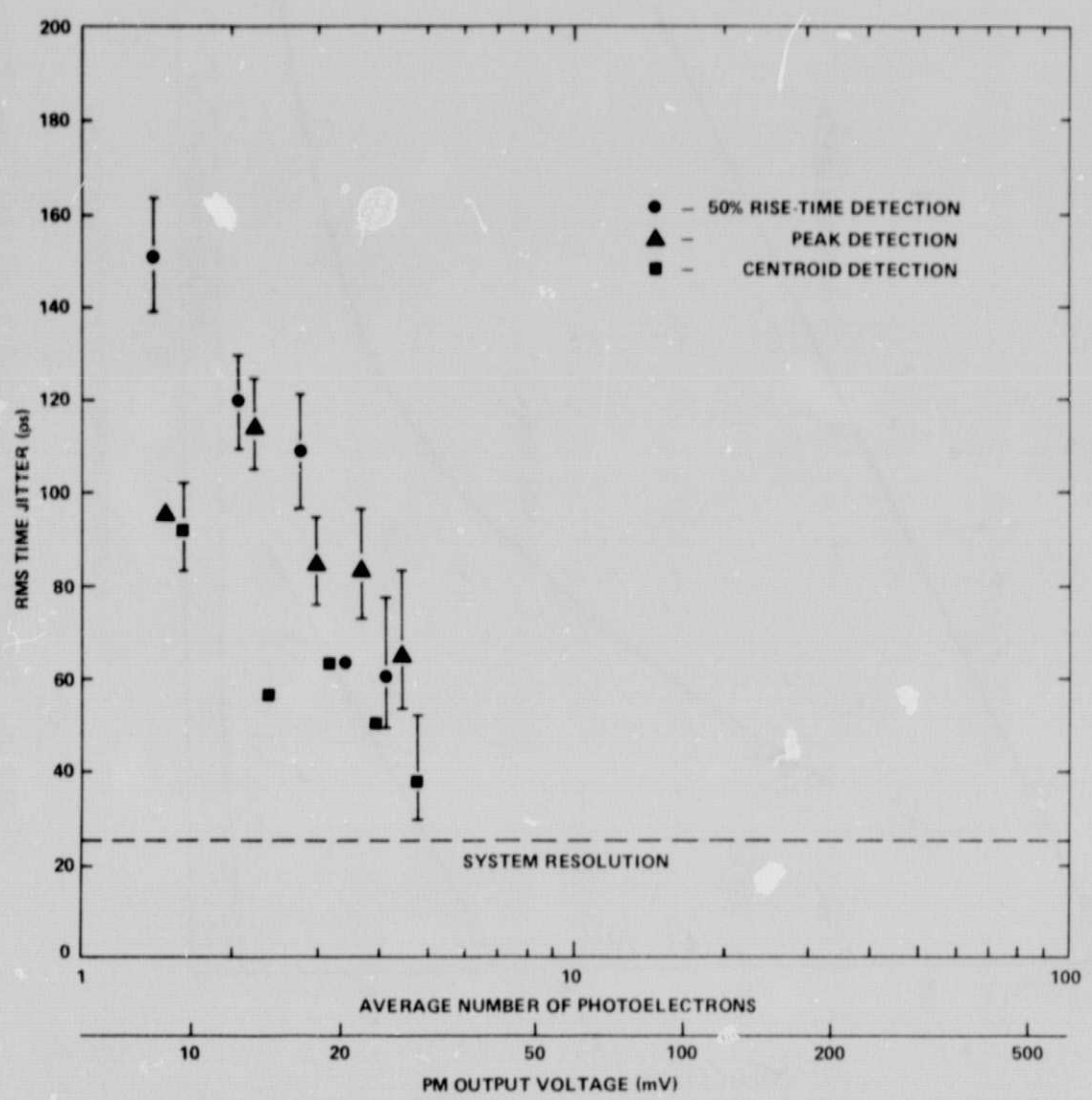


Figure 25. Rms Time Jitter versus Pulse Amplitude for Varian 152S.10P with Detection Strategy as a Parameter

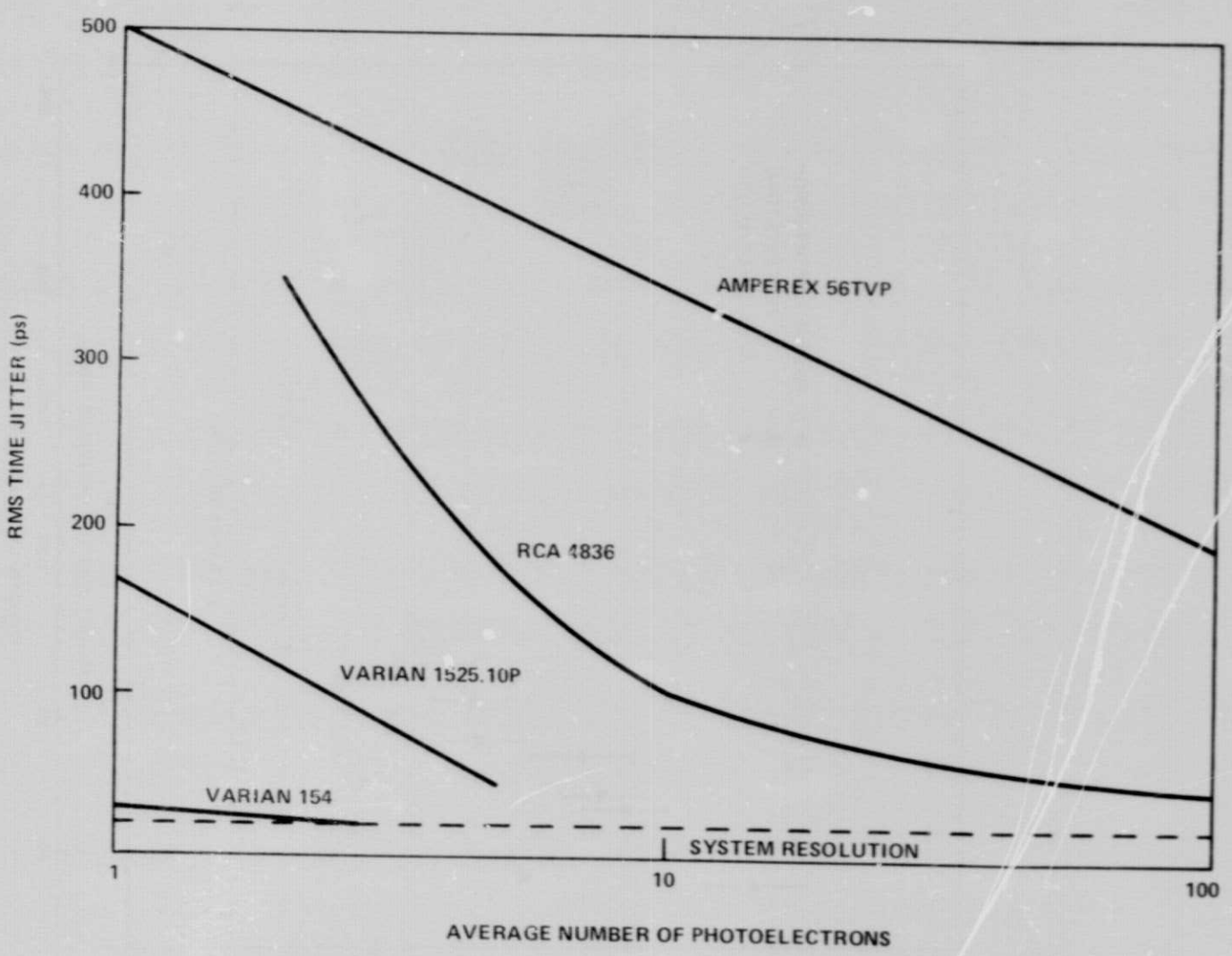


Figure 26. Comparison of Photomultiplier rms Time Jitters

was constant for all signal levels, the time jitters measured for larger anode pulses have a higher signal-to-noise ratio than those for small anode pulses. This effect tended to broaden the transit-time spread for low output signals more than for higher output signals and hence increased the downward slope of the time-jitter curves in the low photoelectron region. Since all other photomultipliers tested had either faster response times or higher gains than the RCA 4836, the residual amplifier noise did not significantly broaden the other transit time-jitter measurements.

For each photomultiplier, the average transit time was measured as a function of signal level. These measurements showed modest variations in average transit time over the 1- to 100-photoelectron range. Closer examination revealed, however, that the changes observed were mainly caused by a small pulse-amplitude-dependent average-time bias in the waveform digitizer. Such changes could be attributable to amplifiers within the waveform digitizer that are operating in a slightly nonlinear region. Further work is in progress to correct this instrumentation characteristic.

Dark-Count Spectra

During testing of the photomultipliers, large multielectron dark counts have sometimes been noted. These dark counts are believed to originate either from residual gas ions bombarding the photocathode or from cosmic-ray interaction with the photocathode window.[5]

The system used for measuring the dark-pulse spectra was described in Reference 1 and is shown in figure 27. This system measures the dark-pulse amplitude distribution for different photomultiplier average anode currents. Of the photomultipliers evaluated, only the two static crossed-field and the Varian 152S.10P electrostatic photomultipliers showed a significant number of multiphotoelectron dark counts.

Figure 28 shows the dark-pulse distributions for the Varian 154A/1.6L for average anode currents of 5, 50, 500, 2000, and 10,000 nanoamperes. These curves show a sharp decrease in the number of dark counts beyond the single photoelectron level and indicate that the multiphotoelectron distribution does not change as a function of average anode current. These results would imply that mechanism for producing the multiphotoelectron dark pulses is independent of average anode current for this photomultiplier.

Figure 29 shows the dark-pulse spectra for the Varian 154D.6D for average anode currents of 130, 1000, 2000, and 10,000 nA. These curves, which show a much higher multiphotoelectron count rate than that of the other static crossed-field photomultiplier, also show a fast decrease in count rate at the single photoelectron voltage.

Because these static crossed-field photomultipliers are identical except for the composition of their photocathodes, the difference in dark-count spectra beyond the single photoelectron region is attributable to their different photocathode materials.

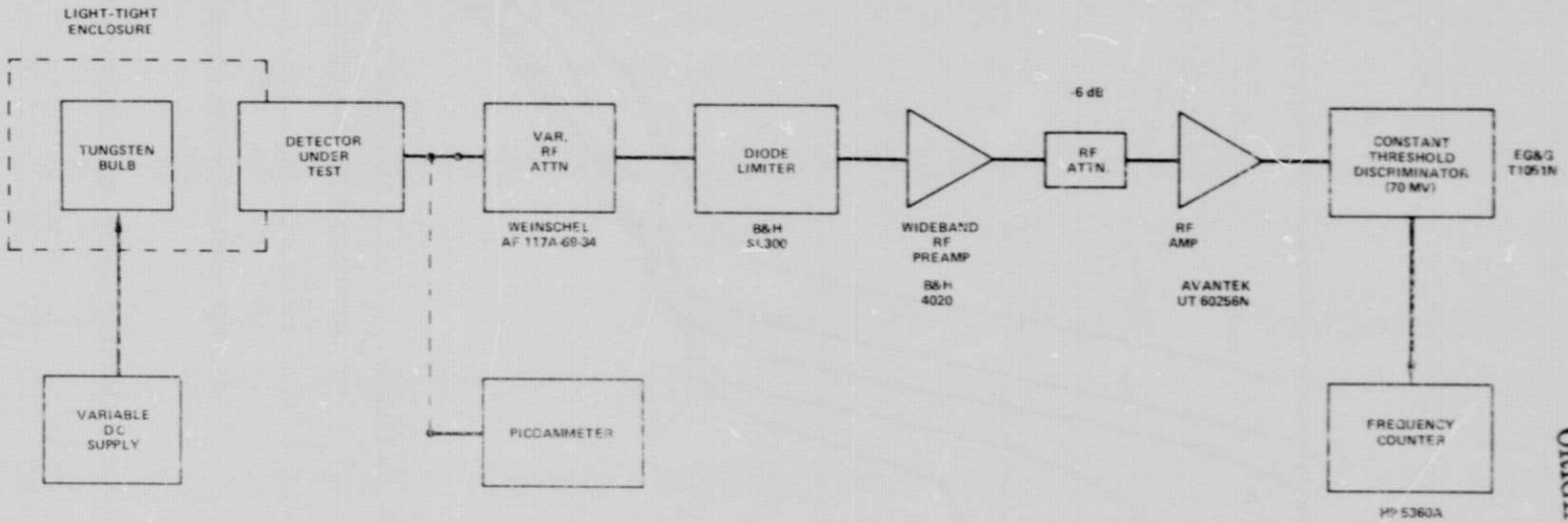


Figure 27. Block Diagram of System for Measuring Dark-Count Spectrum

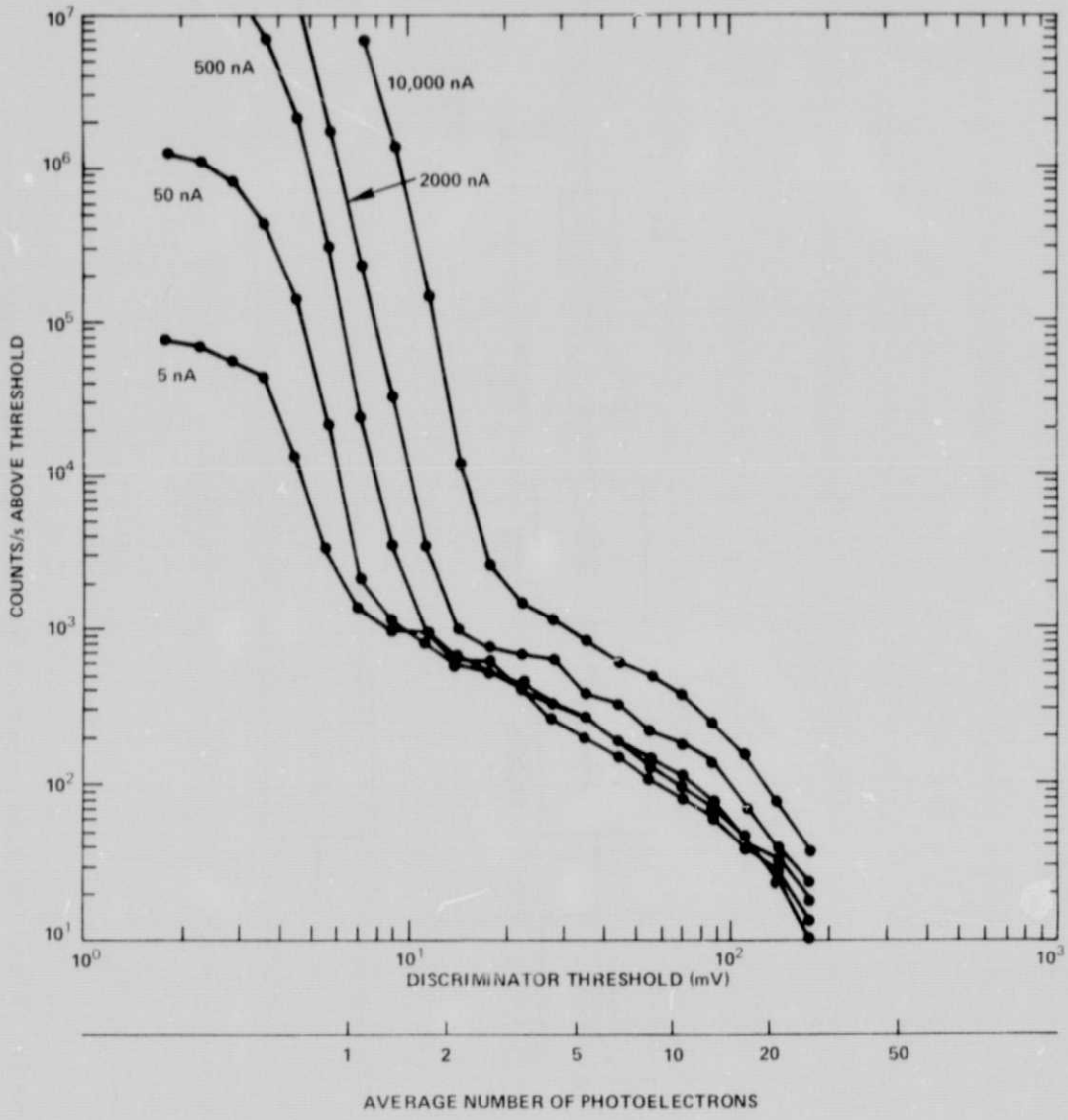


Figure 28. Noise Counts versus Amplitude for Varian 154A/1.6L

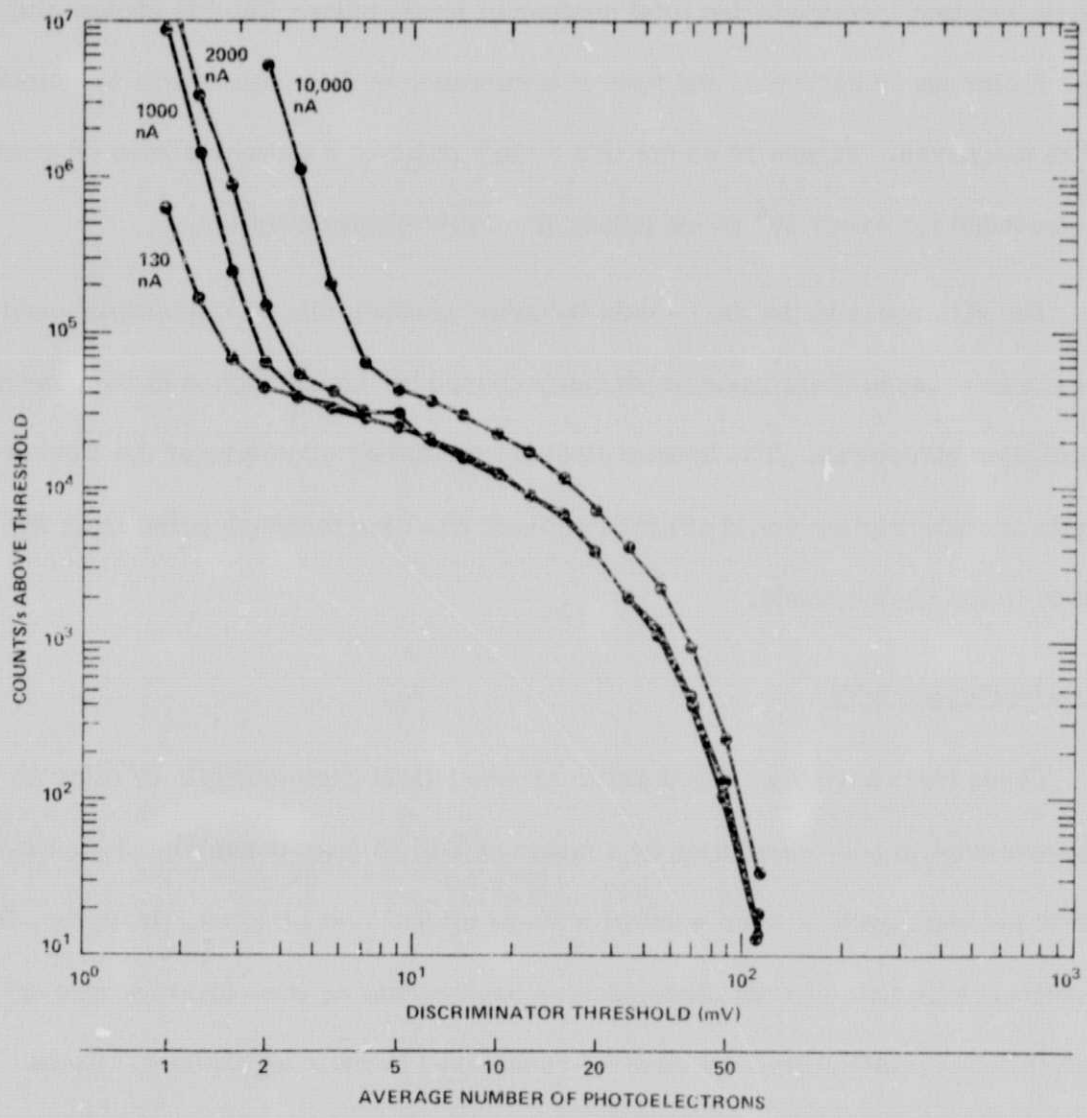


Figure 29. Noise Counts versus Amplitude for Varian 154D.6D

Figure 30 shows the dark-pulse spectra for the Varian 152S. 10P photomultiplier for average anode currents of 0.01, 0.1, 1, 10, 100, and 1000 nanoamperes. The distributions show a sharp decrease in counts above the single photoelectron level for all average anode currents. The appearance of multiphotoelectron peaks at high average anode currents suggests that the large dark-pulse count rate is a small constant fraction of the total number of anode pulses for this photomultiplier. At smaller anode currents, the rate of occurrence of dark pulses was too small to be measured. Figure 30 shows that a dark pulse of 3 photoelectrons or greater is produced for every $10^4$ anode pulses from this photomultiplier.

The difference in the dark-count behavior between this photomultiplier and the static crossed-field types is probably caused by the difference in the electron multiplier structures. The denser electron multiplier structure of the electrostatic photomultiplier would effectively block most ion feedback paths from the anode to the photocathode.

Concluding Remarks

These tests have shown that static crossed-field photomultipliers offer an improvement in time resolution of a factor of 3 to 20 over conventional electrostatic photomultipliers when used with 50-ps optical test sources. However, their relatively high rate of multiphotoelectron dark counts as compared to those of conventional photomultipliers must be considered in their application. These counts can increase the false-alarm rate in laser ranging systems, increase

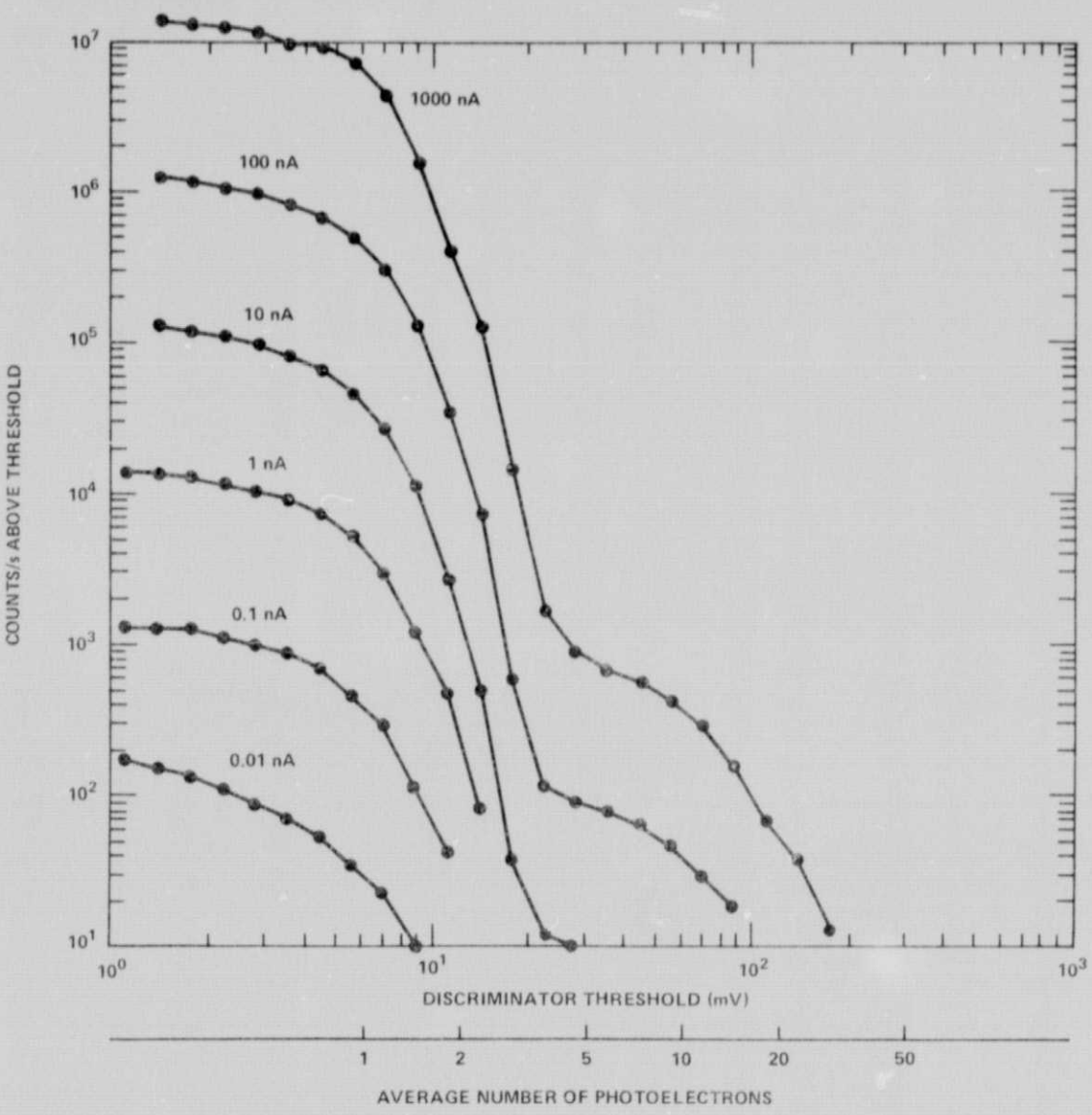


Figure 30. Noise Counts versus Amplitude for Varian VPM152S.10P

error rates in short-pulse laser communications systems, and damage sensitive postdetection electronics.

Acknowledgments

The authors thank Dr. Michael W. Fitzmaurice for valuable discussions and support and Thomas W. Zagwodzki for his ready assistance throughout these tests.

## REFERENCES


1. Abshire, J., and H. Rowe, Systems for Measuring the Response Statistics of Gigahertz Bandwidth Photomultipliers, NASA TM-78029, November 1977.

2. Lo, C., and B. Lescovar, "Performance Studies of the Varian VPM-154D.6D and VPM-154A/1.6L Static Crossed Field Photomultipliers," Lawrence Berkeley Laboratory Engineering Note LBL-6480, June 1977.

3. Amperex Staff, Photomultiplier Tubes - Devices for Nuclear Equipment, Part 6, June 1969.

4. RCA Staff, RCA 4836 Photomultiplier Data Sheet, RCA, Harrison, New Jersey, March 1973.

5. Morton, G., and H. Smith, "Pulse Height Resolution of High Gain First Dynode Photomultipliers," Applied Physics Letters, B (10), 1968.

6. Krall, H., et al., "Recent Developments in GaP (Cs)-Dynode Photomultipliers," IEEE Transactions on Nuclear Science, NS-17 (3), 71, 1970.